Thesis Rieger

April 12, 2023

A search for the Rieger-type periodicity on the Sun-like stars

Eka Gurgenashvili

The doctoral thesis is submitted to the Faculty of Natural Sciences and Medicine, Ilia State University to obtain the doctoral degree: Doctor of Philosophy in Physics

Supervisor: Professor Teimuraz Zaqarashvili
Professor Ansgar Reiners

Ilia state university
Tbilisi, 2023

Abstract

Solar activity undergoes variations over many different timescales. The main periodicity is 11 years, called Schwabe cycle. In addition to the 11-year cycle, shorter periodic variations known as Rieger cycles have been found in solar activity. Observations over several decades showed that the periodicity always appears near Schwabe cycle maxima and permanently changes its value from cycle to cycle. Observations also revealed that the Rieger periods are shorter during stronger cycles and vice versa. The Rieger periodicity is probably connected to the magnetic Rossby waves in the internal dynamo layer, therefore its cycle to cycle variation can be explained by different dynamo magnetic field strengths in individual cycles. Then the dynamo field strength in each cycle can be estimated by the observed periods and the theory of magnetic Rossby waves. This method can be a very useful tool also for Sun-like stars.

Recent space missions (Kepler, CoRoT, TESS) have collected a large stellar database, which allows us to look for Rieger-type cycles in other Sun-like stars. Before looking for the stellar cycles, we examined the total solar irradiation (TSI) in cycles 23-24 from SOHO/VIRGO data. TSI, which includes the combined contribution of sunspots and faculae, is analogous to stellar light curves and hence permits to study the Sun as a star. We found strong peaks around 180 and 115 days in cycle 23, and 170 and 145 days in cycle 24. Using magnetic Rossby wave theory, we estimated the magnetic field strength in the solar dynamo layer as 10-15 kG.

The Rieger period on the Sun is around 5-7 times longer than the rotation period. Therefore we searched for the solar-type stars, that fulfill the same condition. We found a Sun-like star KIC 2852336 from Kepler data, which showed a clear peak near Rieger time scale in addition to the rotation period, making it a potential Rieger-type candidate. We computed the Lomb-Scargle periodogram and a wavelet power spectrum from the light curve. Periods were found at 9.5 days and 60 days. The 60-day periodicity in the stellar light curve is entirely consistent with the solar case. We used several methods to rule out the possible instrumental appearance of the period and confirmed that it is related with the stellar activity. Then, we estimated the strength of the dynamo magnetic field inside the star as 40 kG. It is found that the ratio of the rotation period and dynamo field strength has the same value for the star and the Sun.

1 Introduction

1.1 The Sun

The Sun is a 4.5 billion-year-old G2V yellow star - a typical dwarf star of medium size, age, temperature, and brightness. The Sun is a giant ball made of hydrogen, helium and other chemical elements. Figure 1 shows the solar structure, which consists of the interior and the atmosphere.

Internal structure of the Sun includes the core, the radiative zone, and the convective zone. The core temperature is 15 million Kelvin, at which matter is in a plasma state. Thermonuclear reactions take place in the core and hence it is a source of solar thermal energy. The energy generated in the core is trapped in the next layer, called the radiative zone. The radiation energy is transferred by absorption and emission of light in this zone. The density in this layer gradually decreases, although it is still so dense that it takes about 100,000 years for light to reach the surface. Therefore, this layer acts as an insulator, because it helps the core to maintain a high temperature. Above the radiative zone is the convection zone, where the energy/light emitted from the core is transported primarily by convection. Hot matter rises from the base of the layer, cools down and returns back forming convection cells. The surfaces of convective cells are seen as photospheric granules. A thin layer between the radiation and convection zones is called the tachocline, where the solar magnetic field is thought to be generated.

The solar lower atmosphere consists of the photosphere and chromosphere. The photosphere is the Sun's visible surface, which is the coldest 500 km thick layer of the Sun, with a temperature of about 6000 Kelvin. Here, the radiation cools the matter from the convection zone that reaches the surface.

The next layer of the atmosphere is the chromosphere, where the plasma temperature starts to rise up slowly. Strong magnetic fields in active regions are expressed in the form of arches in the chromosphere. Active regions last for weeks, while the number of sunspots and active regions varies over the famous Schwabe cycle 11-year period. Between the chromosphere and the corona, there is a transition region where temperature rises rapidly from 20 000 K to 1 million K.

The last layer of the atmosphere is the corona, which can be formally divided into the inner and outer corona. The existence of high coronal temperature of 2 million Kelvin is still an unresolved issue in solar physics. The coronal plasma would cool down in several tens of hours due to the radiation and the thermal conduction without an external heating source. This source can be located in the photosphere, where the dense and dynamic convection contains more than enough energy for the coronal heating. The problem is how to transport the energy upwards and how to dissipate there to heat the plasma. Closed magnetic field in form of coronal loops mainly dominates the corona above sunspots, while the open field lines are seen in coronal holes. High temperature coronal plasma leads to the flow of particles, the solar wind. Matter escapes rapidly from the coronal holes and generates low-density fast solar winds. But the active regions of closed magnetic field lead to the high-density slow solar wind. The outer corona extends over great distances, even beyond the Earth, which was predicted in 1950 by the observations of comets. Parker (1958) developed a theoretical model in which the flow of particles from the Sun played a significant role in the coronal dynamics. His theory was confirmed by satellite observations in 1960 when a solar wind was discovered.

1.2 Solar activity

The activity of the Sun has been observed through sunspots for nearly four hundred years. The Sun is characterized by 11 years of activity, which means that once every 11 years, the level of its magnetic activity, as well as the number of

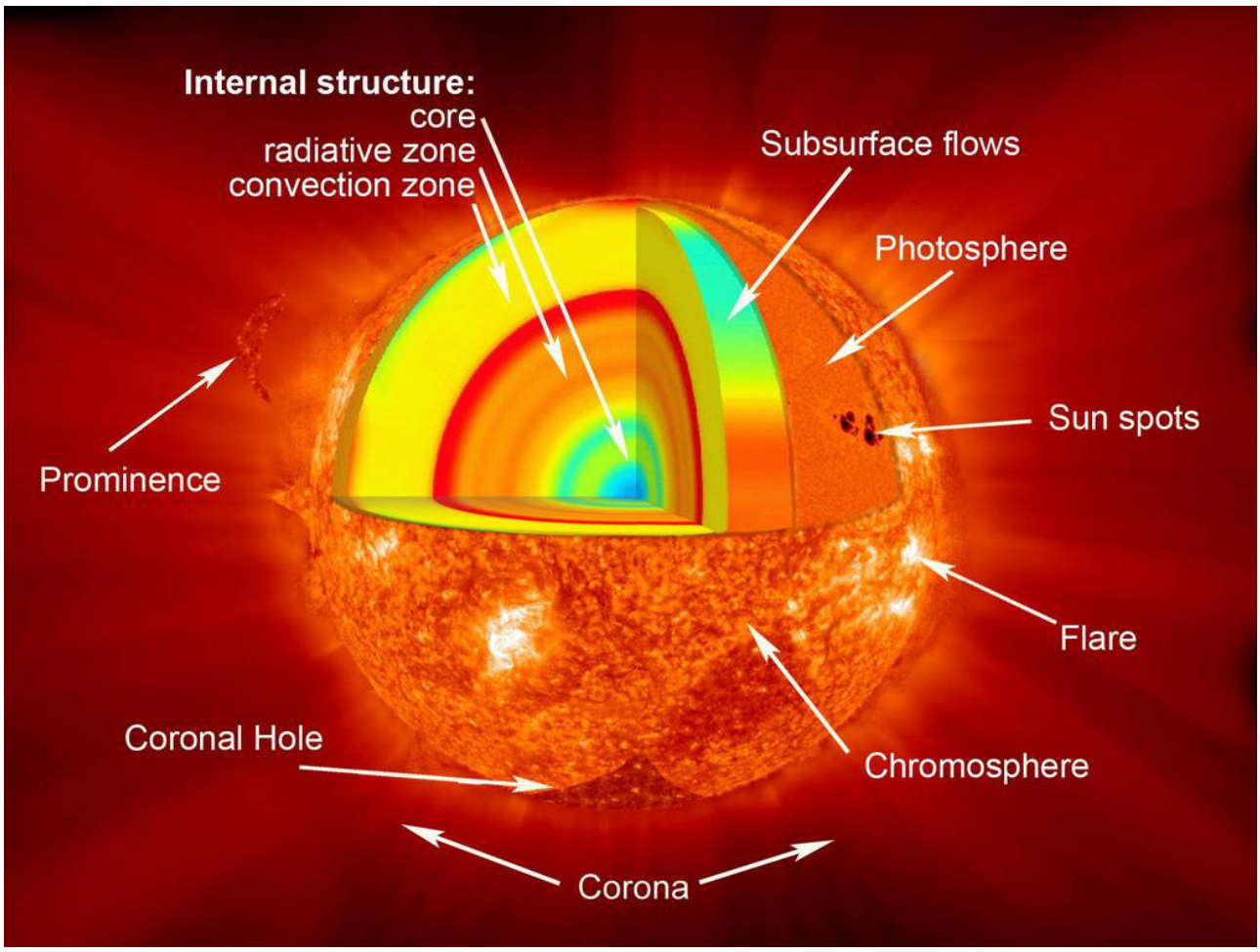

Figure 1: The structure of the Sun: the core, radiative and convective zones, photosphere, chromosphere and corona. Credit to Nasa.gov (https://www.nasa.gov/mission$_pages/sunearth/science/Sunlayers.html$)

the associated high-energy solar events (such as flares, coronal mass ejections (CME), etc.) reach the maximum and then decrease again. Increased activity leads to the enhanced solar ultraviolet and X-ray radiation, which has a major impact on the Earth's atmosphere. Solar flares, CMEs and solar energetic particles (SEP) may damage satellites and may threat astronauts in space and airplane passengers on polar flights.

Sunspots are the best indicators of solar activity. They appear at the beginning of each cycle at a latitude of about 35 degrees in the northern and southern hemispheres and then migrate to the equator when the cycle progresses. Observations of the Sun over centuries has revealed that the solar activity is characterized by different periodicity, some of which are longer and some of which are shorter. For example, a longer period is the Gleisberg cycle (Gleissberg, 1939), which comprises a combination of approximately 10 solar cycles. There are also other long periods of 1000, 500, 350, and 200 years, based on long-term recordings of the sunspot number and observations of cosmogenic radionuclides (Be10 and C14) (Solanki et al., 2004; Hanslmeier et al., 2013; Zaqarashvili et al., 2015). By combined analysis of isotopes and sunspots, a very low level of solar activity was found during 17th century known as the Maunder minimum (Usoskin et al., 2007). On the other hand, shorter period variations are also observed in solar activity, which were discovered by Rieger et al. (1984) and hence are known as Rieger cycles. Other short periodic cycles observed in solar activity are annual (McIntosh et al., 2015; Gachechiladze et al., 2019) and quasi-biennial (QBO) oscillations (Vecchio & Carbone, 2009; Zaqarashvili et al., 2010).

The solar cycles are related to the magnetic field, which is formed by dynamo action inside the Sun. Most dynamo models involve two main processes: amplification of toroidal magnetic field from the poloidal component due to the

latitudinal differential rotation (the Ω effect) and the generation of poloidal magnetic field from the toroidal one due to fluid cyclonic actions (the α effect). However, the exact mechanism of solar activity still remains an unsolved problem. Different dynamo models (Charbonneau, 2010) predict different locations of the dynamo magnetic field generation. The traditional approach suggests the tachocline as the location of the dynamo, which is a thin layer between rigidly rotating radiative and differentially rotating convective zones. Another models suggest that the dynamo magnetic field is generated somewhere inside the convection zone. The tachocline models lead to the presence of a stronger toroidal magnetic field > 10 kG, which may become unstable and cause magnetic flux to rise towards the surface. On the other hand, the models without tachocline suggest weaker magnetic field of < 10 kG.

The direct measurement of the dynamo magnetic field in the solar interior is not possible. Therefore, even rough estimation of magnetic field strength in the dynamo layer is important as it may test the different dynamo models.

Different activity levels are observed in different hemispheres of the Sun. North-south asymmetry is statistically insignificant, although it becomes quite noticeable in stronger cycles. The asymmetry likely reflects the difference in dynamo magnetic field strength across the different hemispheres, although the mechanism of this asymmetry is not yet known.

1.3 Rieger-type periods on the Sun

The periodicity of 154 days was first discovered in 1984 by Rieger et al. (1984) in γ-ray bursts during a maximum of cycle 21 observed by the Solar Maximum Mission (Figure 2). The periodicity has been found during the last few cycles in many activity indices, such as X-ray flares (Dennis, 1985; Bai and Sturrock, 1987; Kile and Cliver, 1991; Dimitropolou, 2008), solar flare energetic electrons (Dröge et al., 1990), sunspot group numbers (Lean and Brueckner, 1989; Carbonell & Ballester, 1990; Carbonell and Ballester, 1992; Lean, 1990; Oliver et al., 1998; Ballester et al., 1999), type II and IV radio bursts (Verma et al., 1991), type III radio bursts (Lobzin et al., 2012), the microwave (Kile and Cliver, 1991) and proton (Bai and Cliver, 1990) flares. Furthermore, Rieger periodicity of about 152-158 days was also found in the data associated with strong magnetic fields (Ballester et al., 1999; Krivova and Solanki, 2002). Lean and Brueckner (1989) found that the periodicity was presented in the sunspot blocking function, in the 10.7 cm radio flux, and in the number of sunspots. At the same time, its presence was statistically insignificant in the plages. These observational results lead to the conclusion that the Rieger period is not only related to flare activity but also with the compact magnetic field structures. Therefore, the periodicity should be related to the internal layer where the solar magnetic field is generated.

Various authors studied long period appearance of Rieger periodicity during many activity cycles. Lean (1990) investigated cycles 12-21 and concluded that the periodicity appeared near the maxima of the cycles, existed for 1-3 years, and then disappeared. The periodicity was not strictly constant, but it varied from 150 to 190 days. Similar results were obtained through analyzes of sunspot areas by Oliver et al. (1998) and Zaqarashvili et al. (2010). Carbonell & Ballester (1990) studied the existence of Rieger periodicity in sunspot areas in cycles 14-20, which was later extended to the cycles 12-21 (Carbonell and Ballester, 1992). The conclusion was that the Rieger periodicity was clearly seen in strong cycles 16-21, while it was absent in the weak cycles 12-15. The Rieger period was also detected in the Wolf numbers from 1849, the solar flux at 2800 MHz F10.7 from 1947, the number of X-ray flares from 1981, and the number of optical flares in the cycle 21 (Akimov and Belkina, 2012). All the studies confirmed that a 154-day period is not a permanent feature of solar activity, but varies from cycle to cycle.

Rieger periodicity is also found in historical data of early cycles. For example, 150-d period was found in Aurora data during the cycle 3, but not during the cycle 4. Silverman (1990) tried to study Aurora data in the 16th and 17th centuries and found the periods of 158 and 182-185 days, respectively. Ballester et al. (1999) analysed the sunspot group numbers and found a period of 158 days in the solar cycle 2. The Rieger periods, observed in different indices during different cycles, are summarized in Table 1.

The physical mechanism of the Rieger periodicity is not yet known. Various mechanisms have been proposed to explain the properties of this periodicity. Ichimoto et al. (1985) suggested that this periodicity is related to the storage time scale of a magnetic field in the solar convection zone. Bai and Sturrock (1991) supposed a ”clock” model with a 25.8-day rotation, where a 155-day period is the sub-harmonic of the fundamental period. Wolff (1992) and Sturrock et al. (2013) tried to explain the periodicity by nonmagnetic r-mode oscillations (i. e. Rossby waves). Lou (2000) introduced large-scale equatorially trapped hydrodynamic (HD) Rossby wave in the solar photosphere as the mechanism for the Rieger period. However, HD approach does not consider a magnetic field, therefore it is unclear how the waves can modulate the solar magnetic activity.

As the periodicity is seen in the activity indices related with the emerged magnetic flux, the magnetic field must

Solar cycle	Time interval	Flares	Sunspots	Magnetic field	Apparent solar diameter	Solar irradiance	10.7cm radio flux	Plage index	Aurorae
	1683-1718				155[h]				
2	1766-1775		158[r]						
3	1775-1784								150 [j]
9	1842-1845								150[o]
12	1878-1889		145 [t]						141–150[o]
13	1889-1901		185.6 [t]						
14	1901-1913		190 [s]						146 [o]
15	1913-1923		190 [s]						
16	1923-1933		158 [s] 163 [r]						
17	1933-1944		160 [s] 162 [r]						
18	1944-1954		160 [s]						
19	1954-1964		157 [s] 153 [r] 159 [i]						
20	1964-1976		166 [s] 159 [i] 159 [i]				159 [i]		
21	1976-1985	154[k] 158[m] 152 [l] 153[e] 154 [b] 154[d]	160[s] 159 [i] 159 [i]	163[p]	155 [n]	157[u]	159 [i]	159[i]	
22	1986-1996		181[s]						
23	1996-2008		159 [s]	163[q]					
24	2008-2016		192 [s]						
1-21	1749-1979		155.4 [g]						
12-21	1878-1982		156.1 [t]						
19-20	1958-1971	154[d]							
19-21	1954-1982		155 [i] 155 [i]				155[i]		
20-21	1965-1986	155[c] 152[f] 152[a]							

Table 1: Reported detections of Rieger periodicity (in day) in solar activity indicators. The first two columns indicate the solar cycles and time interval in which the periodicities have been found. The next columns give the indicator used for the detection, namely: flare data, which comprise observations in γ-, X-rays and microwaves, Hα, protons and energetic electrons, and the solar flare index; sunspot data, covering sunspot areas, the Zurich sunspot number, the group sunspot number and the sunspot blocking function; photospheric magnetic flux; the Sun's apparent diameter; the solar irradiance; the 10.7 cm radio flux; the plage index; and Earth's aurorae. The superscripts identify the paper in which the periodicity is reported. a: Bogart and Bai (1985), b: Kile and Cliver (1991), c: Ichimoto et al. (1985), d: Bai and Cliver (1990), e: Dröge et al. (1990), f: Ozguc & Atac (1989), g: Wolff (1983), h: Ribes et al. (1989), i: Lean and Brueckner (1989), j: Vaquero et al. (2010), k: Rieger et al. (1984), l: Bai and Sturrock (1987), m: Kiplinger et al. (1984), n: Delache et al. (1985), o: Silverman (1990), p: Ballester et al. (2002), q: Ballester et al. (2004), r: Ballester et al. (1999), s: Gurgenashvili et al. (2016), t: Carbonell and Ballester (1992), u: Pap et al. (1990). The table is adopted from Zaqarashvili et al. (2021) and it is this thesis author's contribution to the paper.

Cycle Number	Time interval	Period Total	Period North	Period South
12	1878-1889	145	160	145
13	1889-1901	185	168	187
14	1901-1913	146	150	145
15	1913-1923	190	171	185
16	1923-1933	158	160	195
17	1933-1944	160	153	193
18	1944-1954	160	160	175
19	1954-1964	157	158	177
20	1964-1976	166	165	190
21	1976-1986	160	183	158
22	1986-1996	181	180	160
23	1996-2008	159	175	160
24	2008-2016	192	192	140
12–24	1878-2016	160; 192	160	187; 140

Table 2: Columns 3 to 5 give the estimated Rieger periods (in day) from Greenwich Royal Observatory sunspot area data (http:// solarscience.msfc.nasa.gov/greenwch.shtml), obtained for the whole disk and the northern and southern hemispheres separately during solar cycles 12–24. The table is reproduced from Gurgenashvili et al. (2016, 2017) by permission of the AAS. The table is adopted from Zaqarashvili et al. (2021) and it is this thesis author's contribution to the paper.

be included in the Rossby wave scenario. Zaqarashvili et al. (2010) showed that the periodicity might be explained by magnetic Rossby waves in the solar tachocline, which may become unstable due to the combined action of differential rotation and toroidal magnetic field. The unstable harmonics of the Rossby waves can cause a periodic eruption of magnetic flux towards the surface. The dispersion relation of magnetic Rossby waves depends on the magnetic field strength, so a possible change of the dynamo field from cycle to cycle can affect the periodicity.

Rossby waves are large scale planetary waves, which are also known as r-modes in stellar context. The waves arise due to the conservation of total vorticity in the rotating sphere (Rossby , 1939, 1945). Their phase velocity is directed to the opposite of the rotation. They play an essential role in Earth's global weather system at different latitudes. The Rossby waves have been continuously observed in the Earth's atmosphere and oceans. Their frequencies are several times smaller than the Earth's rotation frequency. The hydrodynamic description of Rossby waves is valid in neutral atmospheres, for example, on the Earth. However, astrophysical objects generally have magnetic fields, which eventually have strong influence on the dynamics of the Rossby waves. One can assume that Rossby waves exist in stellar atmosphere and interiors.

Recent observations revealed the presence of Rossby waves in the solar coronal bright points (McIntosh et al., 2017) and near-surface layers (Löptien et al., 2018). On the other hand, the Rossby waves may arise in the dynamo layers and hence may affect the periodic emergence of magnetic flux. Therefore, they can be observed in activity indices like sunspots and faculae.

Rieger periodicity remains one of the unsolved problems of solar physics. Early studies showed that the periodicity occurred only near the maxima of solar cycles. But, not all cycles displayed the periodicity. The early proposed mechanisms could not explain why this periodicity appeared in one cycle but not in another. The periodicity depends on the strength of the solar cycle and, therefore, on the dynamo magnetic field. This hypothesis is also supported because periodicity is seen in the emerging flux, indicating its connection with its deeper layers.

Gurgenashvili et al. (2016) studied long-term sunspot area and sunspot number data during cycles 14-24 using Morlet Wavelet analyses. The analysis showed that the Rieger periodicity was seen in all cycles; however the period was not always 155 days but was changing in the interval of 155-200 days from cycle to cycle. It was shown that the periodicity negatively correlated with the solar cycle strength: shorter periods were observed in relatively stronger cycles and vice versa (Figure 2). This observation explained the appearance/disappearance: the periodicity did not disappear, but it simply changed its value from cycle to cycle. For example, Carbonell and Ballester (1992) showed that the 155 day period appeared only in cycles 16-21 and did not appear in cycles 12-15. Figure 2 shows that the period in cycles 16-21 was about 155-160 days, while it was 185-190 days in cycles 14-15. The cycle strength

likely determines the value of the Rieger periodicity. Therefore, the observed periods in individual cycles can provide information about the cycle strength. As the cycle strength is probably determined by the strength of the magnetic field in the dynamo layer, it is possible to use the observed periodicity to estimate the mean dynamo field strength during individual cycles.

Using the dispersion relation of magnetic Rossby waves and observed Rieger periodicity, Gurgenashvili et al. (2016) estimated the magnetic field strength during cycles 14-24. It was found that during cycles 16-23, which were most stronger cycles in the interval, the dynamo magnetic field strength was about 40 kG. In relatively weaker cycles such as 14, 15, and 24, the estimated field strength decreased to 20 kG. The results of Gurgenashvili et al. (2016) showed that the estimated magnetic field strength favors the tachocline dynamo models rather than the models without tachocline.

Gurgenashvili et al. (2017) used data from the Royal Greenwich Observatory, KSO/SPO Daily Sunspots and Mount Wilson hemispheric Magnetic flux for cycles 19-23 to study the north-south asymmetry in Rieger periodicity. Cycles 19-20 are north-dominated, which means that the northern hemisphere was more active in these cycles, while the cycles 21-23 were south-dominated. Wavelet analysis showed that Rieger periodicity was different in different hemispheres. For example, during the north-dominated cycles, the Rieger period in the more active northern hemisphere was 160-165 days, while it was 175-190 days in the less active southern hemisphere. Similarly, in the south-dominated cycles, the period was shorter, 155–160 days, in more active southern hemispheres, and longer, 175–188 days, in northern hemispheres. Consequently, Rieger periodicity clearly repeats the asymmetry in solar activity.

1.4 Stellar activity

Transit of cold and dark sunspots on the solar disk reduces the brightness, while bright structures, e.g. faculae, increase it. Total solar irradiance (TSI) includes both contributions, sunspot darkening and faculae brightening. TSI has been actively observed by different space missions for the last 4 cycles. In the case of Sun-like stars, we do not have such long term accurate measurements. In such a case, the S-index is used, which measures the stellar chromospheric flux. In the case of the Sun, the magnetic field associated with the active regions as well as the magnetic network, reflects the radiation of the solar chromosphere. Then, the chromospheric radiation is expressed as intensity of singly ionized calcium H and K lines (Ca II H&K). Similar method is used to study the magnetic activity of stars. In the 1970s, Wilson (1968) started the famous H&K project, which aimed to detect solar-like cycles in the chromospheric radiation of Sun-like stars. After 1977, Wilson's observations continued as the Mount Wilson HK program (Baliunas et al., 1995). This project is summarized in the works by Baliunas et al. (1995, 1997). According to observations, the activities of most cold dwarf stars are similar to the Sun, which can be characterised by unevenly distributed magnetically active dark and bright regions.

First measurements of the photometric brightness variability in cold stars started in the 1980s. These observations also included Hyades, a young cluster with 10% of the solar age stars. Upon examining the simultaneous temporal behavior of photometric and chromospheric observations, the measurements showed that young stars become photometrically fainter as their chromospheric emission increases and vice versa. Stars similar to the solar age exhibited solar-like variability by becoming brighter when their chromospheric emission peaks (Radick et al., 1990).

Observations at the Lowell observatory revealed the first apparent annual brightness changes in young Sun-like stars. Like short periodic fluctuations, long-term variability is characterized by changes in average chromospheric activity. Younger stars became brighter when their average activity level decreased and vice versa, hence the chromospheric and photospheric variations did not match. An obvious questions raised whether the relationship between the long-term photometric and chromospheric variability was characteristic only for the stars of Hyades or for other young active stars as well. How do older and less active stars behave? Is the Sun different from such stars?

Observational analyzes of 33 stars were performed at Lowell and Mount Wilson Observatories. The stars were taken mainly from Wilson stars. The most extended observation time was 4 years, which is too short to cover the complete cycles for many stars. However, important information about stellar long-term behavior can also be obtained from this short time series. From these 33 stars, the young active stars repeated the behavior of the Hyades stars. In contrast, the older and less active stars showed sun-like behavior: their brightness changed with the change in chromospheric activity.

The observations led to the conclusion that the activity of cool stars is similar to that of the Sun. Active regions include both bright and dark structures that are unevenly distributed on the stellar surface. The activity of young stars (S-index) is in anti-phase with their brightness variability, while it is in phase for the older stars such as the Sun (Radick et al., 1990).

Vaughan & Preston (1980) presented a study of 486 main sequence F-G-K-M type stars and concluded that the stars are characterized by different levels of chromospheric activity decreasing with age. As a result, there is a deficiency of F-G stars with intermediate activity. In addition, these authors discovered two sequences with a gap called as the Vaughan-Preston gap. Noyes et al. (1984) examined 13 main sequence Sun-like, slow-rotating stars similar to solar age that exhibited a Sun-like long-period chromospheric cycles. Baliunas et al. (1995) studied G0-K5 type stars and roughly divided them according to S-index: young fast-rotating stars with high S-index and old slow-rotating stars with low S-index. Baliunas et al. (1996) used 25 years of records of Ca II H&K chromospheric emission measurements from the Mount Wilson Observatory and compared the ratio between cycle length and rotation period to predictions available from stellar dynamo theory. Baliunas et al. (1997b) divided the periodic variation of stars into three categories. The first category included young rapidly rotating stars with uneven and irregular variability. The second category contained old and slowly rotating stars, which were about 80% of the sample stars. Furthermore, those stars (20%), which did not show any variation, were assigned to the third category. It turned out that solar-like cycles are quite often on stars. The cycle amplitude also depends on stellar mass so that the more massive stars with the same age have lower amplitude cycles than the Sun. But the stars of the same age and lower mass have stronger and more pronounced cycles.

Brandenburg (1998) proposed an interpretation of the relationship between the rotation period, activity level and activity cycle (P_{cyc}) based on Ca II H & K observations, so that the dynamo α-parameter increases with magnetic field strength, contrary to the conventional idea of α-quenching. Next, Saar & Brandenburg (1999) extended the study of photometric cycles from the BY Dra and W UMa systems, which confirmed the results of the previous study that the stars are distributed in two parallel branches on cyclic period-Rossby number (Rossby number is the ratio of the rotation period and the convective correlation or turnover time) diagram. More active stars are mostly on the lower branch, but they fall on the upper branch with increasing age.

Böhm-Vitense (2007) confirmed the existence of inactive (I) and active (A) sequences in stars. There were also A-sequence stars that had a secondary cycle that fell on the "I" branch. The Sun is located between these two sequences, although do Nascimento et al. (2015) found that the Sun is located on a sequence of solar analogs. Oláh et al. (2002) found that nine from ten rapidly rotating stars showed cyclical variations, while six of those seem to vary on two or multiple time-scales (see also (Olàh & Strassmeier, 2002; Messina & Guinan , 2002)). Radick et al. (1998) examined the relationship between photometric measurements and the Ca index for 35 stars. Lockwood et al. (2007) presented an analysis of photospheric and chromospheric variability of 32 main-sequence stars. It was found that the young active stars become fainter when their Ca II emission increases, while older less active stars such as the Sun become brighter when their Ca II emission increases. Oláh et al. (2009) found multiple cycles in only 15 out of 20 stars.

Cyclical activity has been detected in both Kepler and CoRoT missions. Vida et al. (2014) and Ferreira Lopes et al. (2015) found cyclic variations in very rapidly rotating Kepler and in CoRoT 16 F-G-K type stars, correspondingly. In recent years, activity cycles have also been found through asteroseismology (García et al., 2010; Salabert et al. , 2016). Reinhold et al. (2017) found cyclic variations in 3,202 stars from 23,601 samples and the two sequences, especially the active sequence, were strongly questioned.

Rotation of Sun-like stars slows down during evolution, their overall activity level gradually decreases, and regular activity cycles are developed. The evolution of variability in brightness is quite challenging as the balance between dark spots and bright structures is changing through evolution: initially stellar activity starts with the domination of spots, but later bright structures dominate of stellar activity cycles (for the stellar age $\gtrsim$ 2.55 Gyr (Reinhold et al., 2019)). However, on rotational timescales, the spot dominate.

1.5 Rieger-type cycles on the Sun-like stars

The short periodic cycle in the other Sun-like star was first detected in τ Bootis, which was reported to exist for 30 years (Baliunas et al., 1995). τ Bootis has received great attention and has been featured in various papers over the years, confirming 120, 117 and 90-day cycles (Mittag et al., 2017; Mengel et al., 2016; Schmitt & Mittag, 2017). Other short-cycle periods detected by ground based observations were 294 days in binary system (Massi et al. , 2005), 300 days in G5-M4 stars (Distefano et al., 2017), and shorter cycles of less than 1 year in four F-type stars (Mittag et al., 2019).

Detection of Rieger cycles on the other stars is quite challenging due to two main reasons. First, our knowledge about stellar activity is not as good as of the Sun. Second, observation time is limited. Ground based observations are limited by various factors including day-to-night variability, weather, and atmospheric conditions. On the other hand, recent space missions have further extended our knowledge about stars. Various missions, such as Kepler, CoRoT and TESS, have been launched to detect exoplanets; but they also observed hundreds of thousands stars for years giving

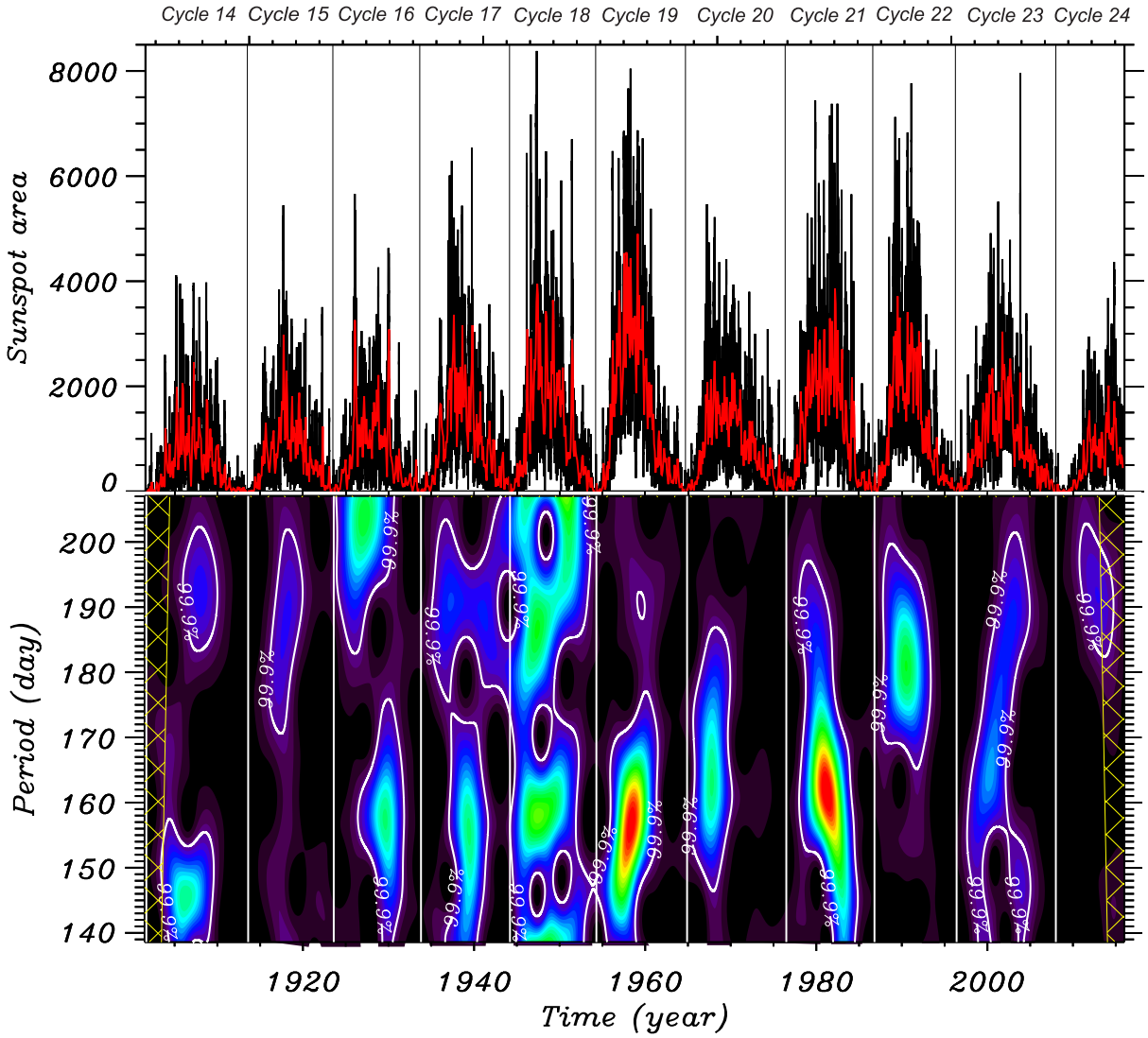

Figure 2: Rieger periodicity during solar cycles 14–24. Top panel: daily and monthly averaged sunspot area data with black and red color, respectively, from GRO data. Lower panel: Morlet wavelet analysis of GRO daily sunspot data. Vertical solid lines correspond to solar activity minimum. White lines encircle the most important powers, above confidence level 99.9%. Adopted from Gurgenashvili et al. (2016)

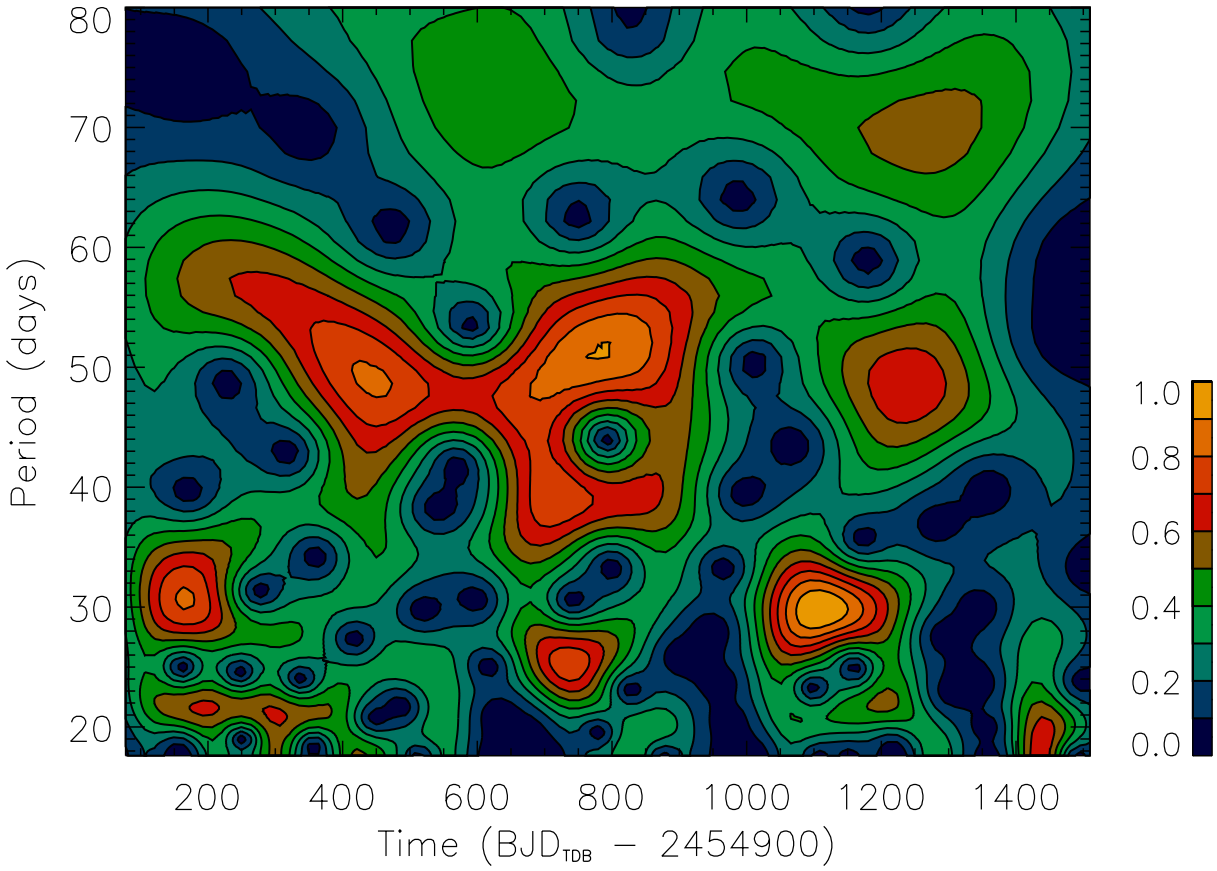

Figure 3: Wavelet analysis of the total spotted area in Kepler-17. Colours orange to dark blue indicate different amplitudes. A 50d and 30d periods are observed in this star. Adopted from Bonomo & Lanza (2012).

unique stellar databases.

Continuous observations by Kepler and CoRoT missions made it possible to observe short periodic cycles on other solar-type stars. For example, CoRoT-2 is a G7-type star with a rotation period of 4.52 days. A period of about 29 days was found on this star, which may correspond to the solar Rieger cycle (Lanza et al., 2009). Another CoRoT F5 dwarf star (HD 49933) with short cycles was also discovered with periods of 120 days (García et al., 2010) and 212 days (Mittag et al., 2019).

There are more discoveries by Kepler, because it had almost 4 years of continuous observations and observed more than 300,000 stars. One of the first stars with short periodicity was a solar analog Kepler-17, a G2V-type star with a rotation period of 12 days, with a hot Jupiter orbiting around. Data analysis showed a short 48-day cycle (Figure 3), which was probably a Rieger-type cycle (Bonomo & Lanza, 2012; Lanza et al., 2019). Several other papers reported Kepler stars with short periods of several hundred days (Arkhypov et al., 2015; Reinhold et al., 2017; Montet et al. , 2017; Arkhypov and Khodachenko, 2021).

Mathur et al. (2014) studied the activity of 22 F-type stars and reported that only two stars displayed the periods of 1400 days and 650 days. Ferreira Lopes et al. (2015) analyzed the CoRoT main sequence F-G-K type stars to find potential stellar activity cycles. The rotation period of these stars was in the range of 0.9-12.9 days. The authors found stellar cycles ranging from 33 to 650 days (See Table 1 in this article for more details).

2 Data

In order to understand stellar activity, it is of fundamental importance to use the Sun as a star analog as we have much more detailed information about solar activity variations. Therefore, two different types of data are used in the thesis. First, the total solar irradiance data is used to search the short period variations in solar activity. Second, the data of Kepler space mission is used to search the short period cycles on other Sun-like stars.

2.1 Total solar irradiance (TSI)

Solar radiation is significant for the Earth and its atmosphere. It was believed that the radiation was unchanged and hence the TSI was called as the "solar constant". However, it turned out that the sunspots and faculae and hence solar cycles affect TSI and consequently it varies with 0.1%. The solar constant was considered as 1365 W/m^2, although more accurate measurements of the SORCE satellite have shown that it is approximately 1360.8 ±0.5 W/m^2.

First attempts of TSI measurements were started in the 1830s by John Herschel and Claude Pouillet, but they did not detected any variations. Later measurements of 1900s also failed to detect a 0.1% variability in TSI. The detailed study of TSI started in 1978 with launching of Nimbus7. TSI has gained even more interest later and continued to be studied by various missions such as ACRIM I (SMM), ACRIM II (UARS), VIRGO (SOHO), ACRIM III (ACRIMSat) and TIM (SORCE) for the last 40 years. Figure 4 shows the TSI observations during different years. As we can see from this figure, several missions measured the TSI simultaneously in several time intervals, which gives an excellent opportunity to make composites. The figure is adopted from Greg Kopp's TSI Page. [1]

The variations in TSI are mainly caused by sunspot and faculae contributions. It is very important to study the relation between the components, as it might give us an important knowledge how the TSI is changing. This can be used for better understanding of the stellar light curves observed by space missions like Kepler. It is believed that the sunspots are the main and more powerful indicators of solar activity, however it turned out that the faculae contribution is also important. Faculae are slightly brighter compared to the environment, although their brightness slightly exceeds (with 0.1 %) sunspot darkening. The faculae usually appear at the latitudes of 40-70° and they migrate towards poles, while the spots appear at the latitudes of 30-35° and migrate towards equator. Polar faculae are small scale magnetic structures contributing to solar cycle. Polar faculae cycle is different and negatively correlates with sunspot cycle. Chapman et al. (1997) studied faculae data for 7.5 year in cycle 22 and found that the mean ratio of faculae to sunspot area was 16.7, which was increased as the cycle progressed. Hence, the faculae had 50% greater influence on solar luminosity than sunspots.

TSI data consists in observational and reconstructed sets.

Observational data sets are:

a) NIMBUS-7 of NOAA (National Oceanic and Atmospheric Administration): daily data exists for 1978 -1993 (Hoyt et al., 1992);

b) ACRIM I (Active Cavity Radiometer for Irradiance Monitoring) on SMM (Solar Maximum Mission): daily measurements exist for 1980 - 1989 (Willson, 1984);

c) ACRIM / ERBS (Earth Radiation Budget Satellite) of NASA: 2 measurements in week for 1984- 2003 (Lee, 1987);

d) ACRIM II on UARS (Upper Atmosphere Research Satellite): daily data exist for 1991-2001 (Willson, 1994);

[1] `https://spot.colorado.edu/~koppg/TSI/`

e) SOHO/VIRGO [2] combines two radiometers (Diarad and PMO6-V) and two sun-photometers, which measure the spectral irradiance on 402, 500 and 862 nm. VIRGO data have much higher quality than the other radiometers. The data are one of the best and continuous, although the data gaps appear on the ascending phase of cycle 23 (Fröhlich et al., 1995).

f) SORCE [3] (Solar Radiation and Climate Experiment) is available from March 1, 2000. Small data gap can be found here due to the battery problems. SORCE instruments measure the full disk TSI and Spectral Solar Irradiance (SSI) data from 0.1 nm to 2400 nm. The measurements are available in daily and 6 hours average formats (Kopp et al., 2005).

g) ACRIM III on ACRIMSAT of NASA: daily measurements exist from 2000 until to today [4] (Willson, 2001);

In order to study the long-term variations of the TSI, one can also use several different reconstructed data sets, which can be foud on MPS webpage [5]:

a) SATIRE-S includes the data of TSI and SSI starting from 1947 ((Yeo et al., 2014). It includes the contributions of faculae brightening and sunspot darkening (here "S" stands for the Satellite era).

b) EMPIRE is an alternative reconstruction of TSI and SSI. Daily data are available from 1947 (Yeo et al., 2017).

c) SATIRE-T includes earlier records of sunspot numbers (1610-1876) and the sunspot area data (Wu et al., 2018; Dasi-Espuig et al., 2016). There is also SATIRE-T2, where the surface flux transport model was used (here "T" stands for the telescope era).

d) SATIRE-M uses the reconstruction of the sunspot number to construct TSI and SSI over the last nine millennia (Wu et al., 2018).

e) Composite of SATIRE-S and SATIRE-T, which are annual means of TSI for the interval of 1700-2012 (Krivova et al. , 2010; Yeo et al., 2014).

In the first paper of this thesis TSI measurements by SOHO/VIRGO are used for the cycles 23-24. VIRGO has some data gaps, especially during the ascending phase of cycle 23. The gaps were filled by SATIRE data.

2.2 Kepler space mission

For the search of Rieger-type cycles on other Sun-like stars the data of Kepler is used in this thesis. NASA's planet-hunter Kepler, named in honor of German astronomer Johannes Kepler, was designed to detect exoplanets. Of particular interest of Kepler were 1-2 Earth size planets in habitable zones of hosting stars. Kepler's scientific goals included to determine orbital parameters, the size of planets, and number of planets in multi-stellar systems etc.

Kepler space mission is a telescope with an aperture diameter of 1 m and a mirror diameter of 1.4 m. During its almost 4-year space odyssey, Kepler observed more than 200,000 stars. The first result appeared within 6 weeks of the start of the scientific operations: Kepler-4b, 5b, 6b, and 8b were among the 5 exoplanets discovered, followed by the discovery of the first planetary system, Kepler-9, with more than one planet.

Kepler searched for exoplanets using the transit method. A transit occurs when the planet passes between a star and an observer. During transit, the planet passes through a stellar disk, and darkening occurs in the stellar light, which is seen in the light curves. Transit is a very useful tool as it can determine the properties of exoplanets: the size of the exoplanetary orbit, the size of the planet (which can be estimated by how much it reduces the stellar irradiation), even the composition of the exoplanet atmosphere, which is very important for habitability.

The Kepler focal plane consists of 25 individual modules. The 4 edge modules are used for fine guiding, while the 21 modules are used for scientific operations. The telescope and field of view of the Kepler spacecraft are presented on the left and right panel of Figure 5.

In 2011, Kepler stopped scientific operations due to the technical problems, but Kepler team managed to solve the problems and revive the spacecraft. Kepler's most important discoveries include the planet Kepler-16b, which orbits two stars; Kepler-47, a multi-planetary system in which planets move around several stars; Kepler-22 b, which is located in the stellar habitable zone; and Kepler-78 b, an Earth-sized planet.

Following the closure of Kepler's first 4-year phase in 2012, NASA decided to extend the mission. Kepler already had 2,300 planetary candidates, and 100 confirmed exoplanets by this time. According to Kepler data, 17% of the stars had an Earth-sized planet.

[2] https://www.pmodwrc.ch/en/research-development/space/soho/#SOHO-VIRGO

[3] http://lasp.colorado.edu/home/sorce/data/tsi-data/

[4] https://asdc.larc.nasa.gov/project/ACRIM%20III.

[5] http://www2.mps.mpg.de/projects/sun-climate/data.html.

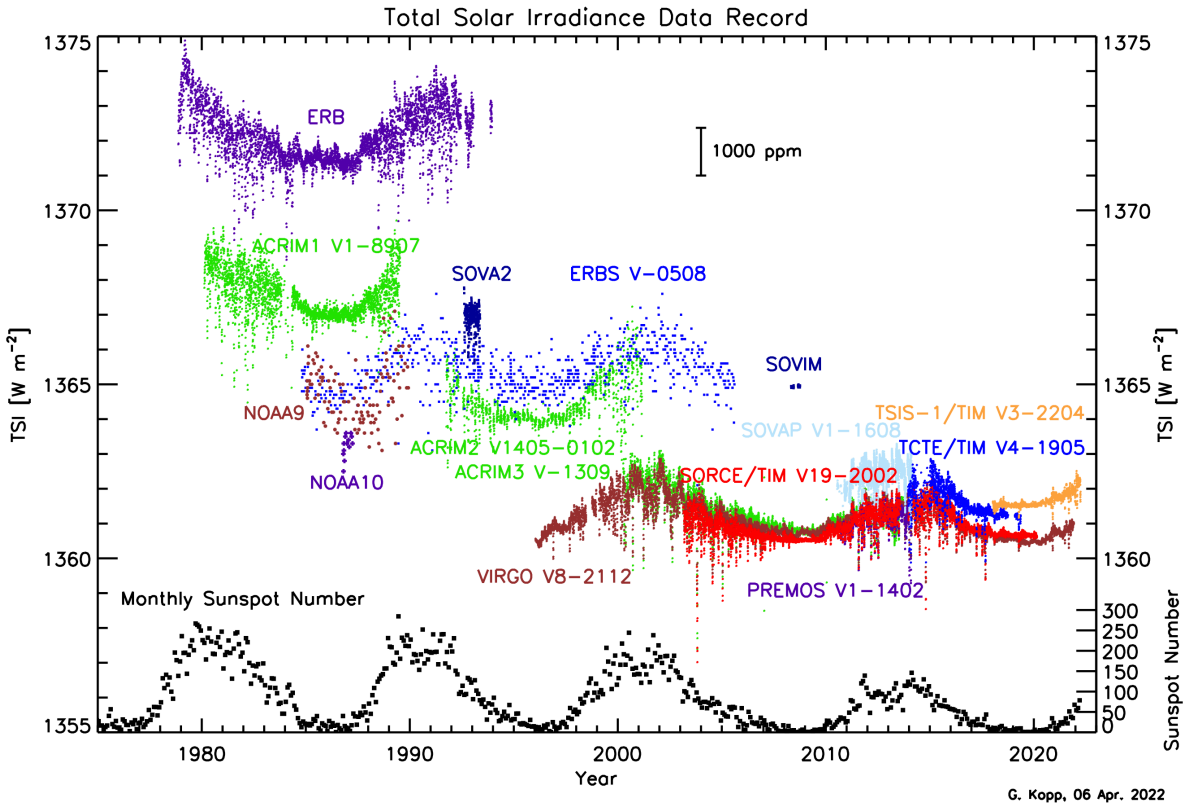

Figure 4: More than 40 years of observation of the total solar irradiance data from various space missions. Different colors correspond to the different spacecraft/instrument, such as ACRIM I-II-III, ERB, NOAA, VIRGO, etc. Black dots below represent monthly sunspot number. The figure is adopted from Greg Kopp's TSI Page.

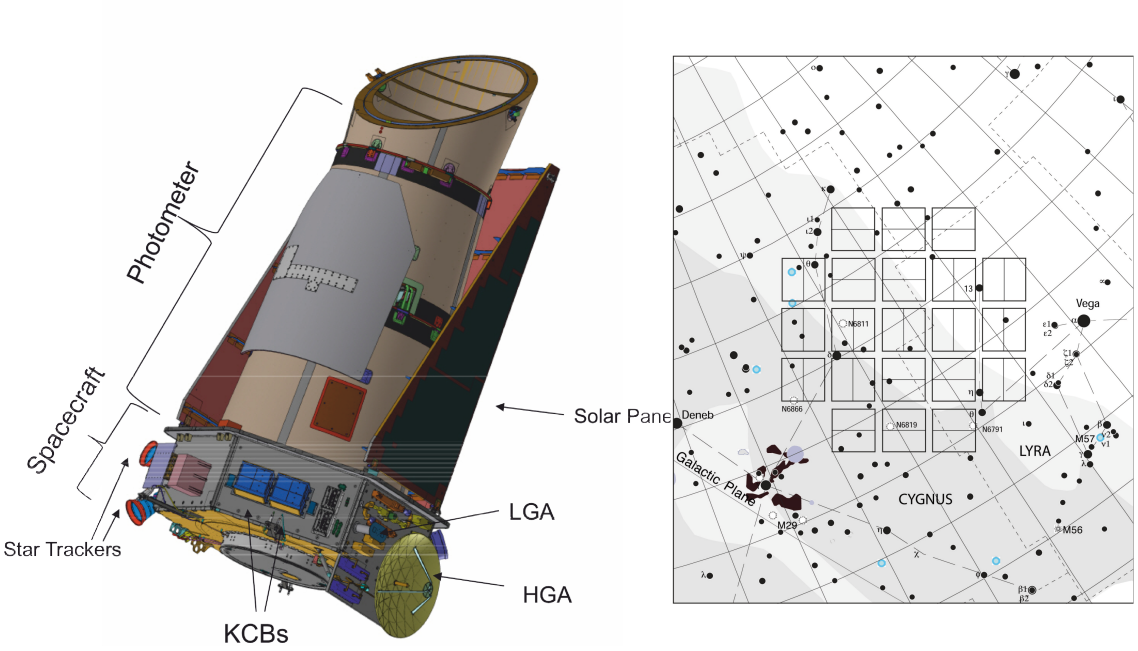

Figure 5: Left panel: The structure of Kepler mission. Right panel: Kepler field of view (FOV).

Kepler has two types of data: Simple Aperture Photometry (SAP) and Pre-search Data Conditioning (PDC) time series. The first one contains strong instrumental trends that need additional corrections. Instrumental trends are mostly removed from the PDC data. Quite rigorous methods often clean PDC data, so that periods above 25 days in stellar light curves are removed. Due to Kepler observational methods and focal plane characteristics, the spacecraft rotates quarterly by 90 degrees, called as the Kepler quarters. During the rotation of spacecraft, positions of observed stars are changed; some are entirely removed from the field of view, while others move to other CCDs that have different characteristic properties and sensitivities. Shifting from one CCD to another shows jumps in the data that need to be removed to avoid computational errors in data analysis. So, one should avoid these jump effects, which can easily be done by matching the median values between successive quarters. During the transition from one quarter to the next, the data often show a few-day gap. In some stellar light curves, this gap lasts for a whole quarter due to the peculiarities of Kepler observations (The star falls on a dead CCD every 4th quarter). Therefore, a lack of data is usually problematic during analysis. We use GLS (Zechmeister & Kürster, 2009) analysis, which is effective for unevenly spaced data. The second method we use is Wavelet analysis (Torrence and Compo, 1998), for which data gap is problematic. Therefore, we try to select the stars in which the data gaps are minimal and then fill them with averages.

3 Results

3.1 Paper I: Rieger-type periodicity in the total irradiance of the Sun as a star during solar cycles 23-24

Gurgenashvili, E., Zaqarashvili, T.V., Kukhianidze, V., Reiners, A., Lanza, A.F., Oliver, R., Reinhold, T.

The contents of this section are identical to the printed version of Gurgenashvili et al., A&A, Vol. 653, A146, 2021. DOI: 10.1051/0004-6361/202141370
Contributions to the paper: E.G. analysed data, produced the results and provided the main scientific interpretation.

Abstract

Total solar irradiance allows for the use of the Sun as a star for studying observations of stellar light curves from recent space missions. We aim to study how the mid-range periodicity observed in solar activity indices influences the total solar irradiance. We studied periodic variations of total solar irradiance based on SATIRE-S and SOHO/VIRGO data during solar cycles 23-24 on timescales of Rieger-type periodicity. Then we compared the power spectrum of oscillations in the total solar irradiance to those of sunspot and faculae data to determine their contributions. Wavelet analyses of TSI data reveal strong peaks at 180 days and 115 days in cycle 23, while cycle 24 showed periods of 170 days and 145 days. There are several periods in the sunspot and faculae data that are not seen in total solar irradiance as they probably cancel each other out through simultaneous brightening (in faculae) and darkening (in sunspots). Rieger-type periodicity is probably caused by magneto-Rossby waves in the internal dynamo layer, where the solar cyclic magnetic field is generated. Therefore, the observed periods in the total solar irradiance and the wave dispersion relation allow us to estimate the dynamo magnetic field strength as 10-15 kG. Total solar irradiance can be used to estimate the magnetic field strength in the dynamo layer. This tool can be of importance in estimating the dynamo magnetic field strength of solar-like stars using light curves obtained by space missions.

Introduction

The recent NASA space missions Kepler (Borucki et al., 2010) and Transiting Exoplanet Survey Satellite, (TESS, Ricker et al. (2014)) , along with ESA's Convection, Rotation and planetary Transits mission (CoRoT, Baglin et al. (2008)) collected a huge store of information on the basic properties of stars and exoplanets. These missions have provided the light curves for hundreds of thousands of stars, which allows us to gain new insights into stellar interiors using asteroseismology, as well as into stellar activity based on the time modulation of the curves. Stellar light curves may reveal stellar rotation periods (Nielsen et al., 2013; Reinhold et al., 2013; McQuillan et al., 2014) and short-term activity cycles (Ferreira Lopes et al., 2015; Reinhold et al., 2017). To understand stellar rotation and activity, it is of fundamental importance to use the Sun as a star analog since it provides much more detailed information on solar rotation and activity variations.

The analog for stellar light curves is the total solar irradiance (TSI). The variability of solar irradiation was first found after the launch of the Nimbus 7 mission in 1978. Subsequently, radiometers on board different satellites, such

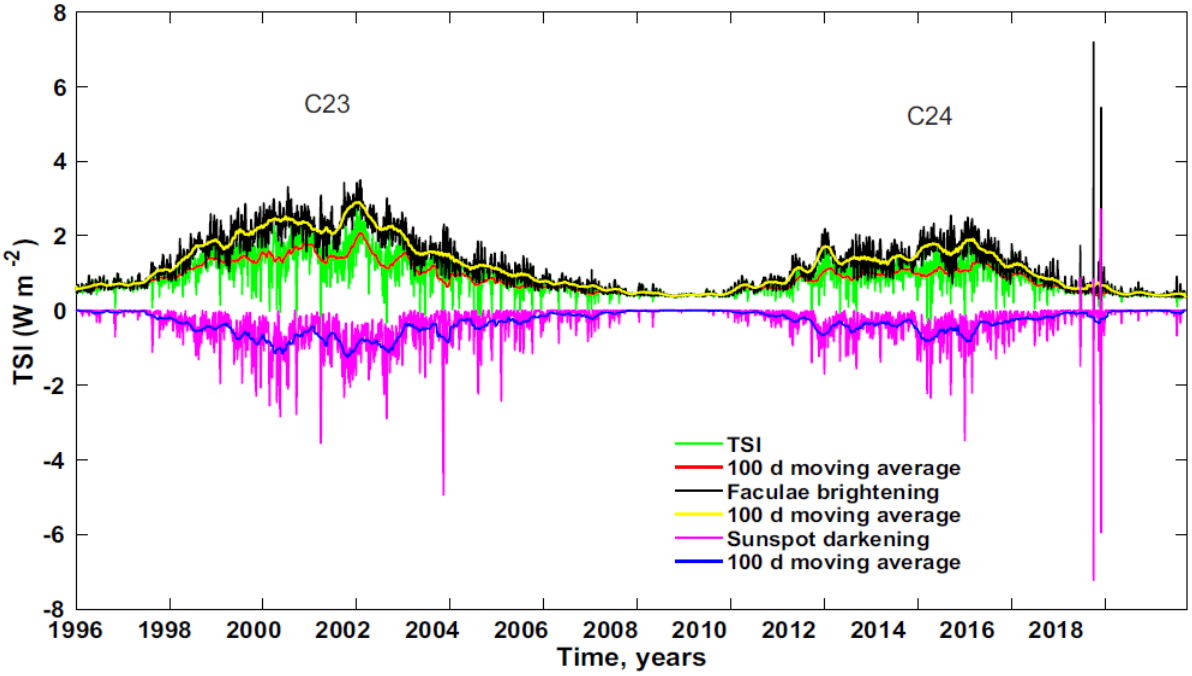

Figure 6: Total solar irradiance (green line) during solar cycles 23-24 from SATIRE-S data in units of W m^{-2}. Red curve shows 100-day moving average of TSI. Black line corresponds to the faculae brightening (with yellow curve as the 100 day average), while the purple line shows the contribution of the sunspot darkening (blue curve as the 100-day average).

as Solar Maximum Mission (SMM) ACRIM-I, NOAA-9, NOAA-10, SOHO/VIRGO, and SORCE/TIM continuously measured the solar bolometric flux (Hathaway, 2010). The variations in the proxies for solar activity (sunspot number; total sunspot area) from the Maunder minimum up through today has been reconstructed using different methods (Krivova et al. , 2009, 2010; Yeo et al., 2014, 2017; Dasi-Espuig et al., 2016; Wu et al., 2018). Using solar full-disc magnetograms and continuum images, Yeo et al. (2014) reconstructed the daily variation of the solar irradiance from 1974 to 2013, using the Spectral And Total Irradiance REconstructions model (SATIRE).

The irradiance observations show that solar brightness changes over different timescales, ranging from several minutes to years. The temporal variation of the TSI is mainly caused by solar magnetic field effects, including sunspot darkening and faculae brightening.

It is important to study the relation between sunspots and faculae, as it has the potential to deliver vital knowledge of how the TSI changes, which can be used to better understand the stellar light curves observed by Kepler. Sunspots and faculae are the most significant contributors to solar activity. Sunspots appear as dark spots on the solar surface, where the temperature is significantly lower. In contrast, faculae are brightest structures where the temperature is higher and they can be easily observed at the solar limb and almost invisible in the center of the disk. At the maximum of the solar cycle, the contribution from faculae dominates the sunspot contribution, making the Sun appear brightest at the maximum.

The Rieger-type periodicity of 150-200 days was discovered by Rieger et al. (1984) more than 30 years ago. This periodicity is seen in many indices of solar activity (Bai and Sturrock, 1987; Bai and Cliver, 1990; Lean, 1990; Ballester et al., 2002, 1999; Oliver et al., 1998; Zaqarashvili et al., 2010). Lean and Brueckner (1989) showed that the Rieger period of 155 days is seen in the sunspot blocking function, 10.7 cm radio flux, and the Zürich sunspot number during solar cycles 19-21, but it is absent in plages, where the magnetic field is weak. This may indicate that the periodicity is related to the solar interior, namely with the solar tachocline, where the solar magnetic field is thought to be generated. Zaqarashvili et al. (2010) suggested that the periodicity can be explained by unstable magnetic Rossby waves in the tachocline owing to the latitudinal differential rotation and the toroidal magnetic field, which may lead to the quasi-periodic eruption of magnetic flux towards the surface. It has also been shown that the Rieger-type periodicity is anti-correlated with the solar cycle strength, such that stronger cycles exhibit shorter Rieger periods

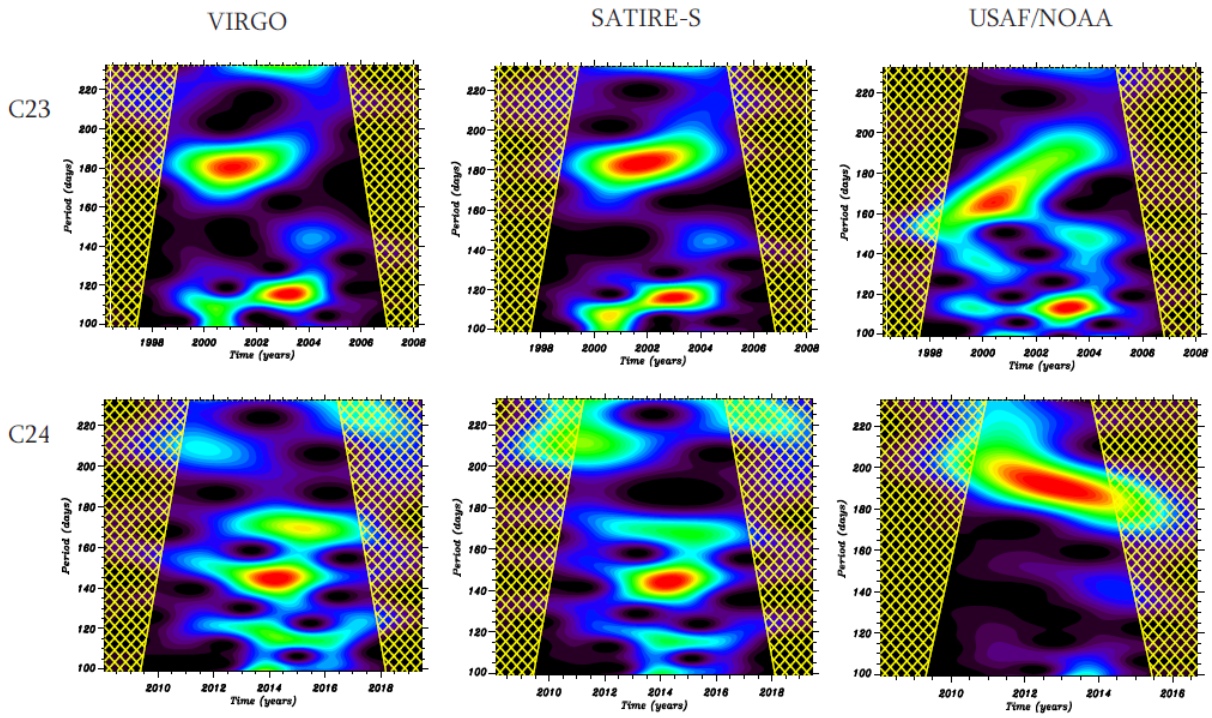

Figure 7: Morlet wavelet analysis in the period range of 100-220 days (Torrence and Compo, 1998). Upper and lower panels correspond to the cycle 23 and 24, respectively. Left panels show the wavelet spectrum based on VIRGO data. Middle panels correspond to the SATIRE data. Right panels display the USAF/NOAA full disk sunspot area data.

(Gurgenashvili et al., 2016, 2017). Therefore, the observed periodicity and dispersion relation of magnetic Rossby waves can be used to estimate the magnetic field strength in the dynamo layer (Zaqarashvili and Gurgenashvili, 2018). Rieger-type periodicity can also be observed in the activity of other stars; therefore, the method may allow for the probing of the dynamo magnetic field on the stars at different stages of evolution.

In order to observe Rieger-type periods on other stars, we can look into light curves provided by Kepler, CoRoT and TESS. The existence of short-term cycles, which are similar to the Rieger periods, was previously reported based on the CoRoT (Lanza et al., 2009) and Kepler (Bonomo & Lanza, 2012; Lanza et al., 2019) observations. However, more observations and detailed analysis of stellar light curves are needed to improve on these results. Prior to a stellar light curve analysis, it is clearly of vital importance to study the periodicity in the total irradiance of the Sun in detail. In this paper, we analyze the TSI data for cycle 23 and 24 and we look for quasi-periodic variations on timescales of Rieger-type periodicities, using the Morlet wavelet transform (Torrence and Compo, 1998).

Data

We used three different data sets, including both observations and reconstructions. For the TSI measurements, we used data from Variability of solar IRradiance and Gravity Oscillations (VIRGO) on board Solar and Heliospheric Observatory (SOHO), combining two radiometers (Diarad and PMO6-V) and two sun-photometers, which measure the spectral irradiance at 402, 500, and 862 nm with 5 nm passbands. To make comparisons with the SOHO/VIRGO TSI data, we used the SATIRE-S reconstruction model (here "S" stands for the Satellite era) from the Max Planck web page [6], which includes the data of the TSI and Spectral Solar Irradiance (SSI) starting from 1947 (Yeo et al., 2014). It combines the contributions of faculae brightening and sunspot darkening.

The VIRGO data has much higher quality than the other older radiometers, however, an almost seven-month gap in the data appears during the ascending phase of cycle 23 (Fröhlich et al., 1995). In order to search periodicities in VIRGO data, we filled the gap with the SATIRE-S reconstruction. For sunspot data, we use the U.S. Air Force/National

[6] http://www2.mps.mpg.de/projects/sun-climate/data.html.

Oceanic and Atmospheric Administration (USAF/NOAA) sunspot area (SA) data [7], that has continuous data for cycles 23-24, without any gaps; however, the data ends in September 2016 and therefore does not cover the most recent years of cycle 24.

Results

Figure 6 shows TSI data using the SATIRE-S reconstruction. Total solar irradiance includes the contributions from different sources, mainly from faculae and sunspots. Faculae brightening (FB) leads to an increase in TSI, while sunspot darkening (SD) reduces it. Figure 6 shows that the faculae contribution has almost twice as much amplitude as the sunspots in both cycles. Several different timescales are seen in the TSI. First of all, there is a clear modulation of TSI with the 11-year solar cycle. In particular, TSI mainly follows the FB curve, which shows that the solar irradiance is faculae dominated. The second timescale is on the order of 0.5-1.5 years (from the range of the Rieger periodicity to that of the quasi-biennial oscillation) and the third timescale is on the order of solar rotation (~27 d). Here we are interested in searching for the mid-range periodicity in the total irradiance of the Sun.

Figure 7 shows the Morlet wavelet analysis of TSI and sunspot area during cycles 23-24 in 100-220 day period window (the periods are defined with close to 5-day accuracy). The hatched regions on the figure (and on all wavelet figures) show the cone of influence (COI), which means that the wavelet transform is not reliable in this areas (Torrence and Compo, 1998). First of all, we note that the VIRGO (left panel) and SATIRE (middle panel) data show almost identical spectra; therefore, SATIRE data can be safely used for detailed analysis. The wavelet spectra are significantly different in the cycles 23 and 24; thus, we consider the periodicities in both cycles separately.

Cycle 23

Two strong periodicities are seen in both the power spectra of the TSI data and the SATIRE-S model, namely: 180 days and 115 days. The peak at 180 days is in the range of typical Rieger-type periodicity (150-180 days) found previously in the sunspot area data (Gurgenashvili et al., 2016). On the other hand, the peak at 115 days is relatively shorter compared to the typical Rieger periodicities, therefore it is probably related with another branch of periodicity (the shorter period can be explained by another harmonic of Rossby waves; see discussion in Section 4). There is also a weak power near the period of 140 days. In order to compare the TSI variations with the sunspot area, we plot the wavelet spectrum of USAF/NOAA data on the right panel of this figure. A strong peak is clearly seen at 115 days, however, the strong power is absent at the period of 180 days. Instead, there is a strong peak near the period of 165 days. We can note the weak peak at 180 days, but it has much less power than the one shown at 165 days. Gurgenashvili et al. (2017) showed that cycles with substantial north-south asymmetry generally display two periodicities corresponding to hemispheric activity. The shorter periodicity is usually revealed in the more active hemisphere. The cycle 23 was south-dominated; therefore, the 165 day and 180 day periods may correspond to the southern and northern hemispheres, respectively. The upper panels of Figure 8 show the wavelet spectra of hemispheric sunspot areas in cycle 23. Indeed, north hemispheric data exhibit strong power at around 175 days, while the southern hemisphere shows a result near 160 days. Additionally, the northern hemisphere has a weak peak at 120-125 days, while the southern hemisphere has a strong peak at 115 days. A comparison of the hemispheric sunspot wavelet spectrum (Figure 8) to that of TSI (Figure 7) shows that the long period in TSI (175-180 day) corresponds to the similar periodicity in the sunspot area of the northern hemisphere, while the shorter period in TSI (115 day) corresponds to the similar periodicity in the sunspot area of southern hemisphere.

The SATIRE-S reconstructed data allow us to study the contributions from faculae brightening and sunspot darkening in the TSI wavelet spectra. Figure 9 shows the wavelet spectra of the faculae brightening and sunspot darkening separately. Several interesting features can be seen in this figure. First, the strong periodicity of 180 days revealed in TSI corresponds to the sunspot contribution as it is not seen in faculae data. Second, another strong peak at 115 days in TSI spectrum is seen in both sunspot darkening and faculae brightening; therefore, it probably results from the joint action of faculae and sunspots. Finally, the two periods of 140 and 165 days, which appear in the faculae and sunspot data, are totally absent in the TSI spectrum. The possibility is that the oscillations cancel each other when TSI variations are considered. To verify this explanation, we fit the following function both to the facular brightening and the sunspot darkening:

[7] http://solarscience.msfc.nasa.gov/greenwch.shtml.

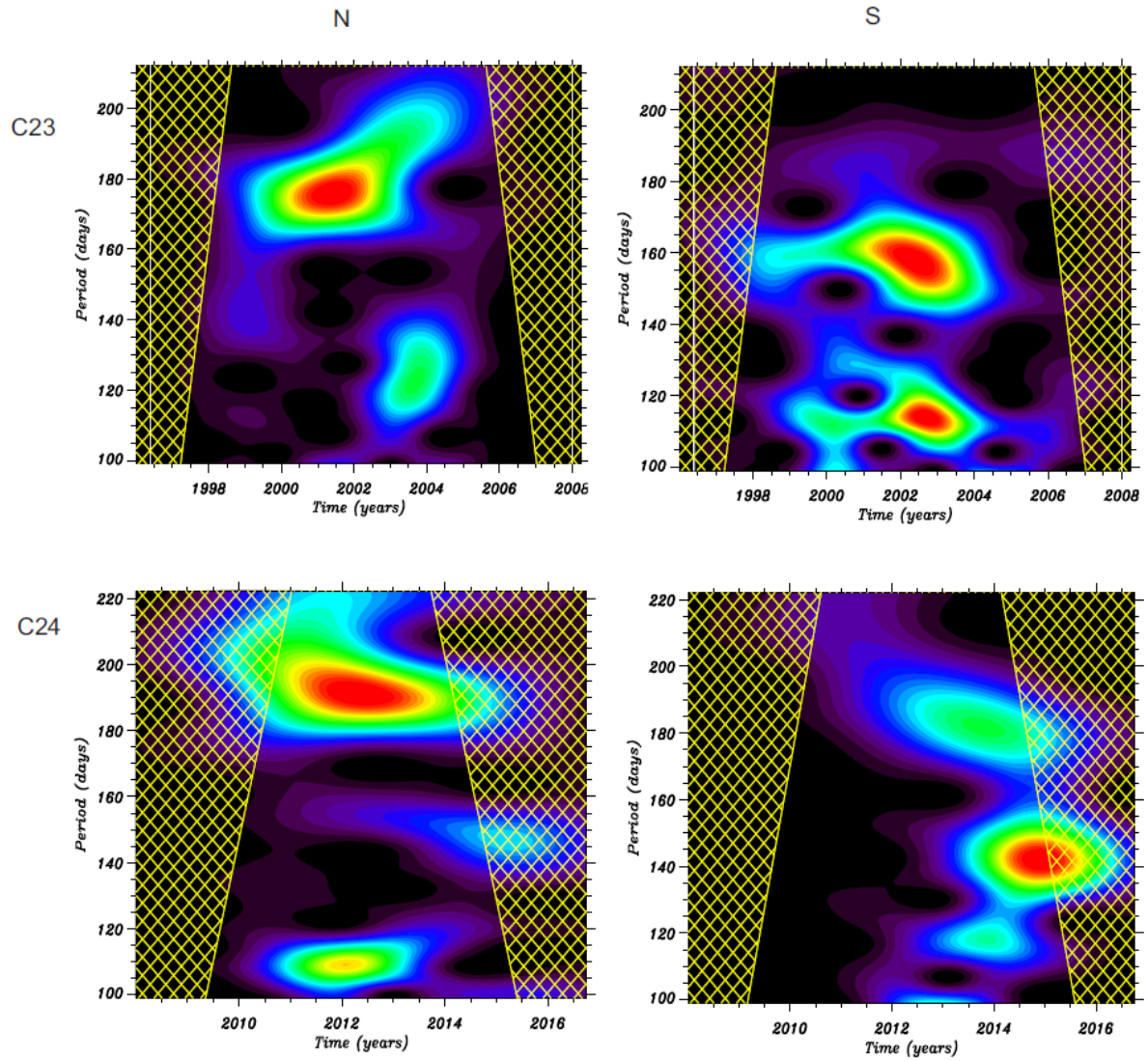

Figure 8: Wavelet spectra of hemispheric sunspot area data during solar cycles 23 (upper panels) and 24 (lower panels) in the period range of Rieger periodicity (100-200 days). Left panels: Northern hemisphere, right panels: Southern hemisphere.

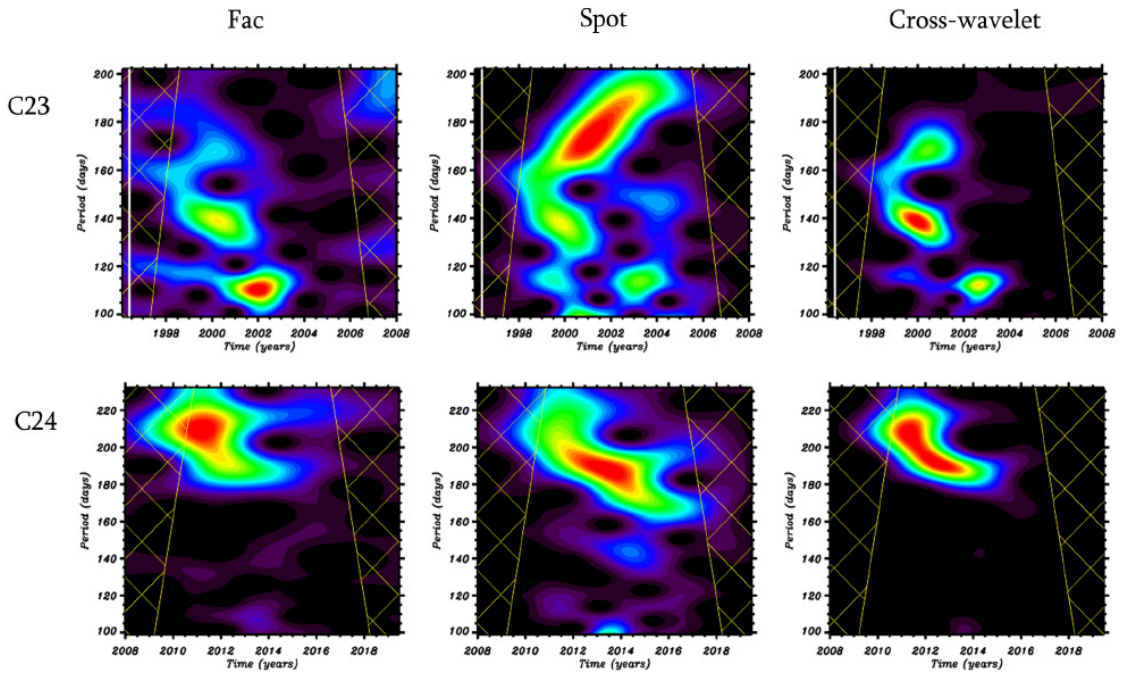

Figure 9: Faculae brightening and sunspot darkening contributions in wavelet spectrum of TSI in the period range of Rieger periodicity (100-200 days) in solar cycles 23 (upper panels) and 24 (lower panels). Left and middle panels show the faculae and sunspot contributions respectively, while the right panels show the corresponding cross-wavelet powers.

$$A\cos\left(\frac{2\pi}{P}t+\phi\right)+C, \tag{1}$$

where A (in W/m^2), P (in days) and ϕ (in radians) are the amplitude, period and phase of the sinusoidal component, respectively, while C is a constant offset and t is the time. The function fitting was done with the MPFIT library (Moré , 1978), using the IDL implementation by Markwardt (2009) [8]. A fitting is done for the raw data, with the following restrictions imposed on the fit parameters: $A > 10^{-5}$, to avoid $A = 0$, which would result in just fitting a horizontal straight line to the data, P fixed and $|\phi| < \pi$. For the 140 d periodicity, the fit was performed for the interval of 1998-2003, when the oscillations were seen in both the faculae brightening and the sunspot darkening. The results are: $A_{FB} = 0.1004$, $\phi_{FB} = 1.163$, $C_{FB} = 2.111$ for the faculae brightening and $A_{SD} = 0.0936$, $\phi_{SD} = -1.975$, $C_{SD} = -0.706$ for the sunspot darkening; P is set to 140 d and is not allowed to vary. The result of the fit is shown in Figure 10.

The phase difference, $|\phi_{FB} - \phi_{SD}|$, equals $3.138 \approx \pi$, hence the two oscillations are in anti-phase during the interval and cancel out because their amplitudes are very similar. This explains why the 140 d periodicity is present simultaneously in the faculae brightening and the sunspot darkening, but is absent in the TSI. The same analysis has also been performed for the 165 d periodicity for the interval 1997-2003 and it was found that $|\phi_{FB} - \phi_{SD}| = 2.535$. Therefore, the absence of this periodicity in the TSI cannot be explained by the cancelation in anti-phase of faculae brightening and sunspot darkening oscillations. We argue that this periodicity is not visible in the TSI wavelet diagram because of its low power and the fact that it is masked by the much stronger 180-day sunspot darkening periodicity.

We did a similar analysis for the 115 d periodicity during the interval of 1998-2006, when the oscillation was seen in both indicators and also in the TSI. The resulting parameters are $A_{FB} = 0.0588$, $A_{SD} = 0.0600m$ and $|\phi_{FB} - \phi_{SD}| = 4.074$. The values of the offsets are $C_{FB} = 1.781$ and $C_{SD} = -0.583$, in agreement with the values of the means. The phase difference is sufficiently different from π, which shows that the two oscillations do not cancel each other out in the TSI. Thus, the presence of this periodicity in the TSI wavelet diagram is also explained.

[8] `http://purl.com/net/mpfit`

Cycle N	VIRGO	SATIRE	fac	spot	SA	SA N	SA S
C23	180	180		180	160	175	160
	115	115	115	115	115	125	115
C24	170		210	185	190	190	180
	145	145				110	115

Table 3: Most significant periods (d) obtained from different data sets (VIRGO/SOHO, SATIRE-S, USAF/NOAA sunspot area (SA), faculae and sunspot contributions). The periods are defined up to a 5-day accuracy.

We also performed cross-wavelet analysis for sunspot darkening and faculae brightening. The cross wavelet is used to more closely examine the relation between the two time series (Torrence and Compo, 1998), in our case the faculae and sunspot contributions in TSI. It is based on the use of complex variables and allows us to calculate the cross-wavelet power. The cross-wavelet power is displayed on the upper right panel of Figure 9, which shows that the periods of 115 day, 140 day and 165 day simultaneously exist in sunspot darkening and faculae brightening as it is visually seen on wavelet spectra of both data. All the observed periods are collected in Table 3.

Cycle 24

TSI displays several peaks in cycle 24 (see lower panels in Figure 7). Strong oscillation power is located at the periods of 170 days, 145 days and 115-120 days. Another weaker peak is seen around 210 days. The peak at 170 days is in the range of typical Rieger type periodicity, while other peaks are out of the range. Wavelet spectrum of full disk sunspot area data shows a strong, broad peak at 180-210 days, a weaker peak at 140 days and a very weak peak at 110 days. It is of importance to check the periodicities in the sunspot area of different hemispheres. The lower panels of Figure 8 show the wavelet spectra of hemispheric sunspot areas in cycle 24. The northern hemisphere shows the broad peak at the period of 190-210 days and weaker peak at 110 days, while the southern hemisphere displays the broad peak at 180-190 days and weaker peak at 120 days. There is a strong peak at 145 days, but almost outside the cone of influence.

The lower panel of Figure 9 shows the wavelet spectra of the faculae brightening (left) and sunspot darkening (middle) from SATIRE reconstruction data for cycle 24. It can be seen that the strong periods of 170 days and 145 days in the TSI wavelet spectrum correspond to the sunspot darkening. The strong peak at 190 days in sunspot darkening is probably canceled by a corresponding period in faculae brightening when we look into the TSI. The weak peak at 210 days in the TSI is probably caused by faculae brightening. The oscillation at 115-120 days in TSI wavelet spectrum is probably generated by weak peaks at sunspot darkening.

We followed the same procedure as for cycle 23 with the 190 d periodicity and fit the function of Eq. (1) to the facular brightening and the sunspot darkening in the periods of 2010-2016. The resulting amplitudes are $A_{FB} = 0.1086$ and $A_{SD} = 0.0857$, while the phase difference is $|\phi_{FB} - \phi_{SD}| = 3.073$. We see that the oscillations are in anti-phase in both data, which leads to its cancelation in the TSI. The cross-wavelet power on the lower right panel of Figure 9 shows the simultaneous existence of 190-220 day oscillations in sunspot darkening and faculae brightening, as it is visually seen in their wavelet spectra. All observed periods are collected in Table 3.

In general, it can be seen that the sunspot contribution in the oscillation spectrum of TSI in the range of Rieger periodicity is stronger than the contribution of the faculae. Hence, the periods in TSI are mostly determined by the periods found in sunspot data.

Discussion and conclusions

Total solar irradiance can be considered as a light curve of the Sun as representative of a star for the purposes of this study. Therefore, a detailed investigation of temporal variation of TSI is a key point in stellar light curve analysis. Our knowledge of the physical processes in the solar atmosphere and interior is far more exhaustive than that of stellar case. It is of importance to know how these processes influence the behavior of TSI, so that we can could perform a reverse task in the stellar case to find out more about the processes in the stellar atmosphere and interior from the temporal behavior of their light curves. We note that the contribution of the bright structures (faculae and networks) in

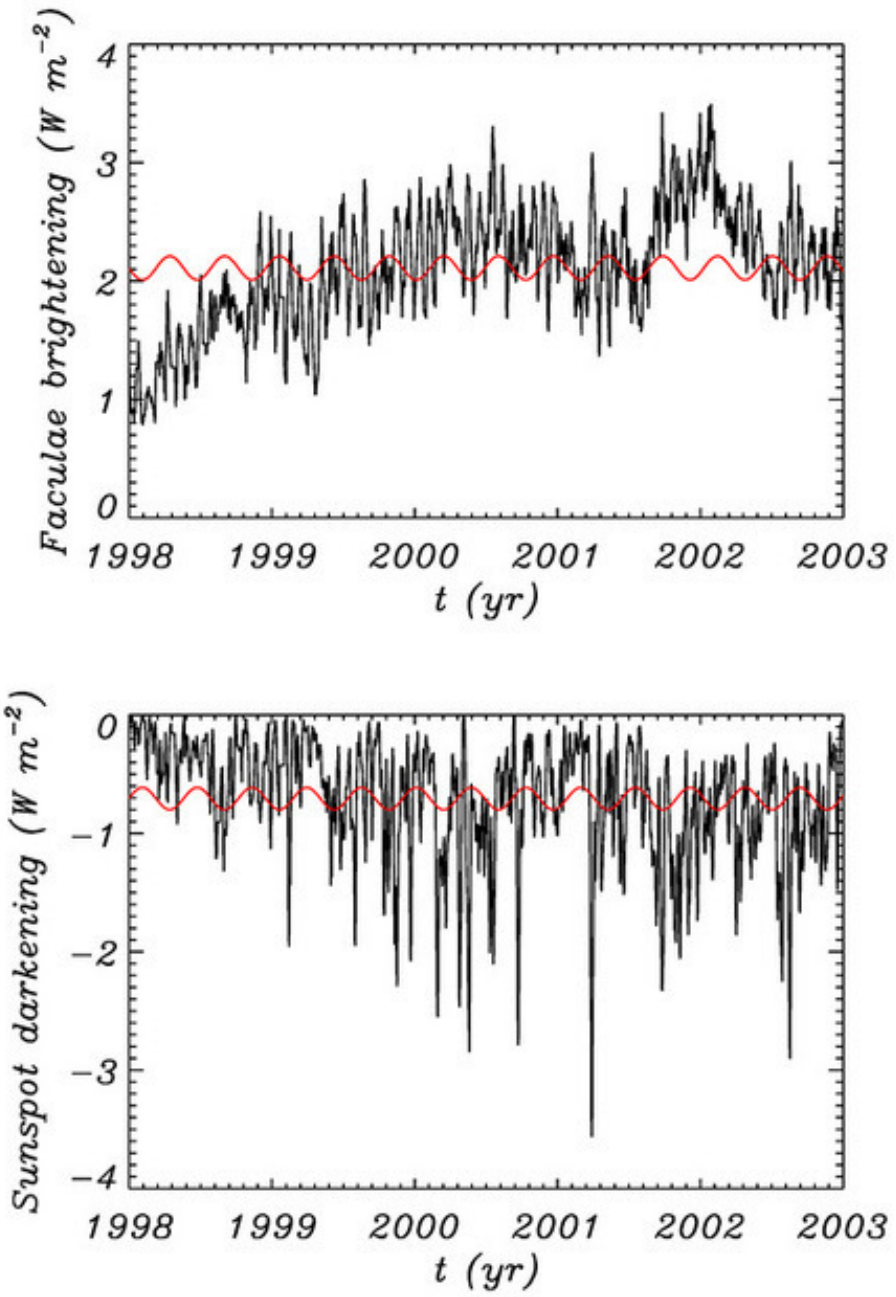

Figure 10: Fitting of a sinusoidal function with the period of 140 days (red curves) defined by Eq. (1) to the raw data of faculae brightening (upper panel) and sunspot darkening (lower panel). We note that the sinusoidal fit here is only used to show the phase relation of the two oscillations and does not intend to model the time series.

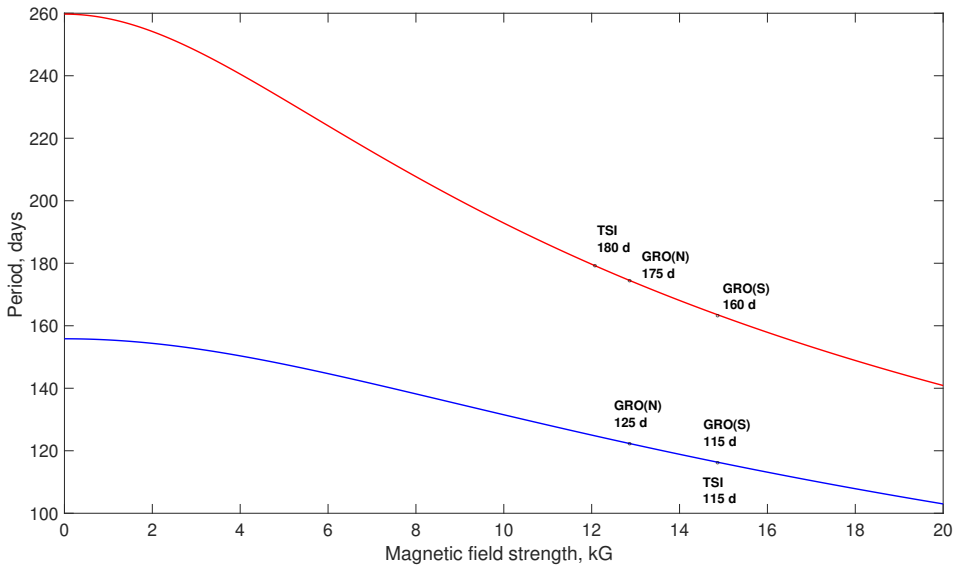

Figure 11: Period versus dynamo magnetic field strength of the magneto-Rossby wave $m = 1$ spherical harmonics with $n = 4$ (red curve) and $n = 3$ (blue curve) plotted according to Eq. (43) from Gachechiladze et al. (2019). The equatorial angular velocity and plasma density in the dynamo layer are assumed to be $\Omega_0 = 2.8 \cdot 10^{-6}$ s^{-1} and $\rho = 0.2$ g cm^{-3}, respectively. The observed periods in different data sets of the cycle 23 are marked by dots on the curves.

the TSI increases at high latitudes, while the contribution of sunspots decreases (Schatten, 1993). Hence, TSI would be different when observed from different inclination angles. Nèmec et al. (2020) also showed that inclination effects on TSI variability are significant. Therefore, the application of solar model to other stars with different inclination angles must be taken with caution.

Here we studied the dynamics of TSI over timescales of Rieger-type periodicity in the solar cycles 23 and 24 using the wavelet transform. There are several findings that could be of importance in subsequent studies of stellar light curves.

The wavelet spectrum of TSI gives two pronounced peaks at the periods of $\sim$ 180 days and 115 days in cycle 23. The period of 180 days also appears in full-disk sunspot data (see the right upper panel of Figure 7 and the middle upper panel of Figure 9), but not in the faculae data (the left upper panel of Figure 9). On the other hand, the hemispheric sunspot wavelet spectra show that the period is connected to the northern hemisphere. The southern hemisphere displays around 160-day periodicity, which is absent in the TSI. The period of 115 days also appears in full-disk sunspot data, and contrary to the 180 days, it is probably connected to the southern hemisphere (see Figure 8). Another weak peak in the power spectrum of TSI is around 145 days, which is also seen in full-disk sunspot spectrum. Therefore, it is clear that the variations in TSI seem to be determined by sunspot darkening rather than faculae brightening. There are two peaks in sunspot data of the cycle 23 at 165 days and 140 days, which are entirely absent in the TSI spectrum. To understand the reason for the disappearance, we should carefully look into the faculae and sunspot contributions (Figure 9). Cross-wavelet analysis shows that both periods appear in the faculae and sunspot data simultaneously; therefore, faculae brightening and sunspot darkening may cancel each other out in the TSI. Indeed, a fitting of the sinusoidal function to the data shows that the 140-day oscillations are in an anti-phase (Figure 10); therefore, the oscillations have almost no contribution. The oscillations with the period of 165 days in both sets of data are not in the anti-phase, but it is likely that they are not seen in the TSI because of their low power. On the other hand, the period of 180 days has no counterpart in the faculae data; therefore, it can be seen in the TSI spectrum. Another period of 115 days in the TSI spectrum is seen in both the sunspot darkening and faculae brightening. However, the period reaches peaks at different times; therefore it is not cancelled out in the TSI spectrum.

The TSI displays the strong periodicity at 170 days and 145 days in cycle 24, while weaker periods are seen around 210 days and 110-115 days. All these periods are probably connected to sunspot darkening rather than faculae brightening. The period of 190 days seen in the sunspot data is probably canceled in the TSI spectrum due to the same

periodicity in the faculae brightening (see lower panel of Figure 9).

It is very important to understand the physical mechanism, which is responsible for the periodicity in TSI. Rieger-type periodicity is supposed to be caused by the instability of magnetic Rossby waves in the solar dynamo layer due to the differential rotation and toroidal magnetic field (Zaqarashvili et al., 2010). Rossby wave dispersion relation in the simplest nonmagnetic case is:

$$\omega = -\frac{2m\Omega_0}{n(n+1)}, \tag{2}$$

where ω is the wave frequency and Ω_0 is the equatorial angular velocity, while m and n are angular order and degree of corresponding spherical harmonics ($m \leq n$). Therefore, observed periods may appear as harmonics of the rotation period. In the nonmagnetic case, $m = 1$ and $n = 3$ harmonics gives the period of 156 days for the rotation rate of 26 days. This is the same value found by Rieger et al. (1984). However, the observed periods are significantly different from the simple harmonics of the solar rotation period. This is because that the toroidal magnetic field of the dynamo layer, which is supposed to operate below the convection zone, modifies the dispersion relation, so that the period of magnetic Rossby waves depends on the field strength and its latitudinal structure (Zaqarashvili et al., 2021). Therefore, we can estimate the toroidal magnetic field in the dynamo layer using the observed periods and the dispersion relation of magnetic Rossby waves. For the latitudinal structure of the magnetic field, we used the formula $B_{tor} = B_0 \sin\theta\cos\theta$, where θ is the latitude, which resembles the solar dynamo field (it has different signs in different hemispheres and reaches maximum at mid latitudes). Figure 11 shows the period vs magnetic field strength for spherical harmonics of magneto-Rossby waves, with $m = 1$ and $n = 3, 4$ according to the Eq. (43) from Gachechiladze et al. (2019). It was shown that only $m = 1$ harmonics are unstable below the convection zone (Zaqarashvili et al., 2010), therefore, we consider only these harmonics, but with different n. We see that the magnetic field with a strength of 12 kG yields the periods of 180 days and 125 days for the harmonics of $n = 4$ and $n = 3$, respectively. These values nearly coinside with the periods found in TSI of the solar cycle 23 (180 days and 115 days). However, hemispheric sunspot areas display the periods of 175 days and 125 days in the northern hemisphere and the periods of 160 days and 115 days in the southern hemisphere. According to Figure 11, the periods correspond to 13 kG and 15 kG magnetic field strength in the northern and southern hemispheres, respectively. Therefore, if the Rossby wave scenario is compatible with the Rieger-type periodicities, then we can use the TSI oscillations to estimate the toroidal magnetic field strength. As the dynamo theory is believed to be responsible for generation of toroidal magnetic field in the solar interior, then the estimated field strength clearly belongs to the dynamo-generated field. In a similar way, the observed Rieger-type periodicity in the light curves of solar-like stars and the dispersion relation of magneto-Rossby waves may allow us to estimate the magnetic field strength in the stellar dynamo layers. This results in a rather rough estimation, but by using many stars with different rotation periods (i.e., at different stages of evolution), this could provide information on a general feature of magnetic field change through stellar age.

3.2 Paper II: Rieger-type cycles on the solar-like star KIC 2852336

Gurgenashvili, E., Zaqarashvili, T.V., Kukhianidze, V., Reiners, A., Reinhold, T., Lanza, A.F.

The contents of this section are identical to the printed version of Gurgenashvili et al., A&A, Vol. 660, A33, 2022. DOI: 10.1051/0004-6361/202142696
Contributions to the paper: E.G. analysed Kepler light curve, produced the results and provided the main scientific interpretation.

Abstract

A Rieger-type periodicity of 150-180 days (six to seven times the solar rotation period) has been observed in the Sun's magnetic activity and is probably connected with the internal dynamo layer. Observations of Rieger cycles in other solar-like stars may give us information about the dynamo action throughout stellar evolution. We aim to use the Sun as a star analogue to find Rieger cycles on other solar-like stars using Kepler data. We analyse the light curve of the Sun-like star KIC 2852336 (with a rotation period of 9.5 days) using wavelet and generalised Lomb-Scargle methods to find periodicities over rotation and Rieger timescales. Besides the rotation period of 9.5 days, the power spectrum shows a pronounced peak at a period of 61 days (about six times the stellar rotation period) and a less pronounced peak at 40-44 days. These two periods may correspond to Rieger-type cycles and can be explained by the harmonics of magneto-Rossby waves in the stellar dynamo layer. The observed periods and theoretical properties of magneto-Rossby waves lead to the estimation of the dynamo magnetic field strength of 40 kG inside the star. Rieger-type cycles can be used to probe the dynamo magnetic field in solar-type stars at different phases of evolution. Comparing the rotation period and estimated dynamo field strength of the star KIC 2852336 with the corresponding solar values, we conclude that the ratio Ω/B_D, where Ω is the angular velocity and B_D is the dynamo magnetic field, is the same for the star and the Sun. Therefore, the ratio can be conserved during stellar evolution, which is consistent with earlier observations that younger stars are more active.

Introduction

Solar activity has its main periodicity at about 11 years, which is known as Schwabe cycle (Schwabe, 1844). However, the Sun also shows shorter-period variations of 150-180 days (Rieger et al., 1984) that usually appear near solar cycle maxima in the activity indices, which are connected to the global magnetic field (Bai and Sturrock, 1987; Lean and Brueckner, 1989; Carbonell & Ballester, 1990; Oliver et al., 1998). Such a periodicity is probably related to the solar internal dynamo layer, where the large-scale magnetic field is generated. The periodicity was recently explained by magneto-Rossby waves in the dynamo layer, which may lead to the quasi-periodic eruption of magnetic flux towards the surface and hence to the modulation of solar activity (Zaqarashvili et al., 2010, 2021). Therefore, observed periods and theoretical dispersion relations of Rossby waves can lead to the estimation of the solar dynamo field strength (Gurgenashvili et al., 2016; Zaqarashvili and Gurgenashvili, 2018). Using the solar and stellar analogy, similar short-term oscillations in stellar activity can be used to estimate the magnetic field strength in the dynamo layers of stars at different stages of evolution.

To search for Schwabe cycles on other stars, Wilson (1968) started to measure the emission in the Ca II H + K line cores, now known as the Mount Wilson S-index. First results of the measurements showed that several of the 91 targeted main sequence stars displayed cyclic activity (Wilson, 1978). Baliunas et al. (1995) studied the Ca II H & K flux of 111 stars and reported that almost 52 of them showed cycling activity.[9] On the other hand, Baliunas et al. (1997) reported the first detection of short-term periodic variations in other Sun-like stars. After studying three stars, ρ^1 Cancri ($P_{\rm rot}$=42 days, age 5 Gyr), τ Bootis ($P_{\rm rot}$=3.3 days, age 2 Gyr, F7 dwarf), and ν Andromedae ($P_{\rm rot}$=12 days, age 5 Gyr), Baliunas et al. (1997) found a short cycle of 116 days in τ Bootis, which persisted for 30 years. Recently, Mittag et al. (2017), Mengel et al. (2016), and Schmitt & Mittag (2017) observed 120-, 117-, and 90-day variations in the same star. Mittag et al. (2019) found four other F-type stars with rotation periods of 3.45 to 7.73 days that display short-term cycles with periods of < 1 yr.

[9] http://simbad.u-strasbg.fr/simbad/sim-ref?querymethod=bib&simbo=on&submit=submit+bibcode&bibcode=1995ApJ...438..269B

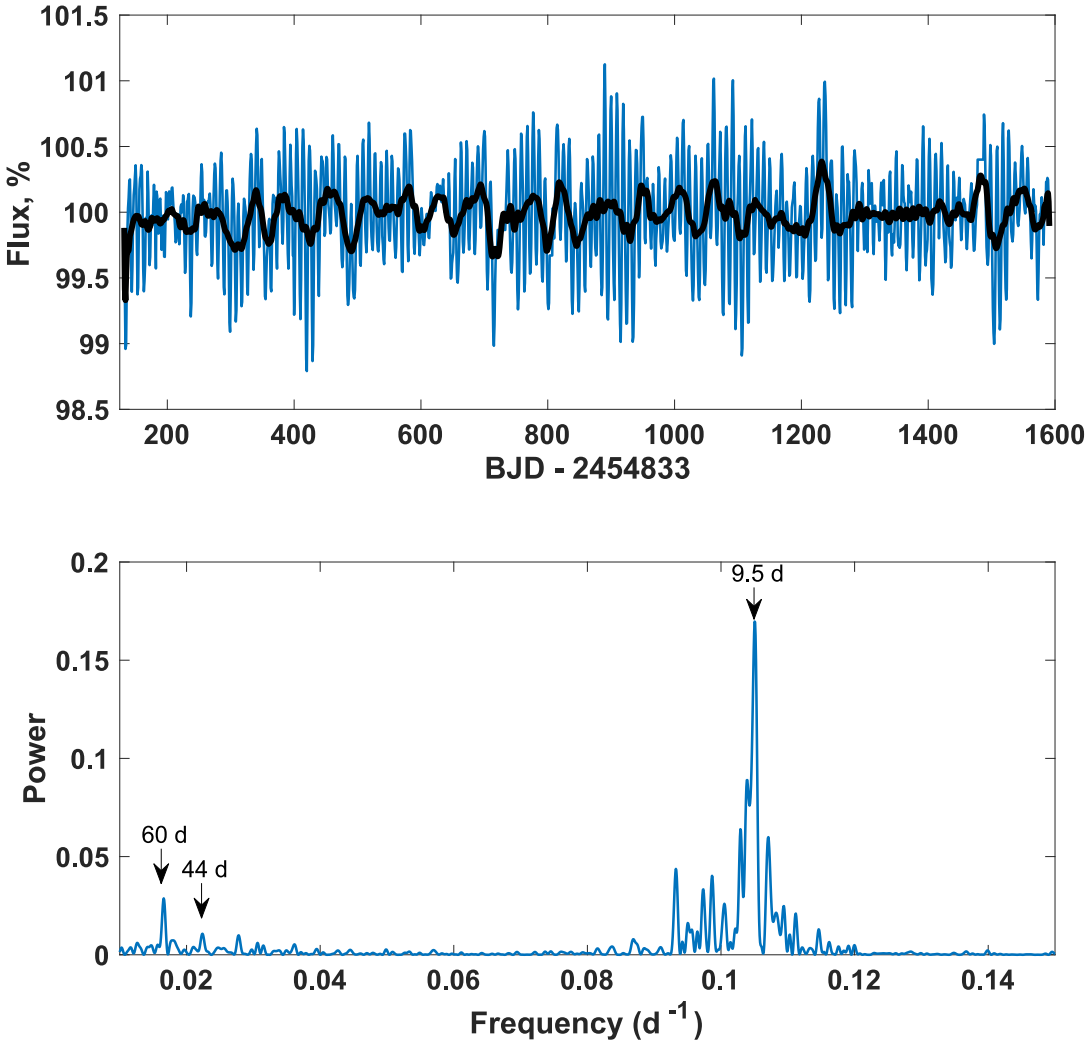

Figure 12: Time series of the Kepler star KIC 2852336 with solid black line denoting the 20-day moving average (upper panel) and the corresponding GLS power spectrum (lower panel). The frequency interval, which includes the periods between 1-90 days, is presented; the rotational periods of 9.5 d, 44 d and 58-61 d (indicated by black arrows), which may correspond to the Rieger cycle, are clearly seen.

The recent NASA space missions Kepler (Borucki et al., 2010) and the Transiting Exoplanet Survey Satellite (TESS; Ricker et al. (2014)) as well as the Centre National D'Etudes Spatiales and European Space Agency (CNES/ESA) mission Convection, Rotation and planetary Transits (CoRoT; Baglin et al. 2008) collected a great deal of information about other solar-like stars. These missions provide light curves, which can be modulated by starspots and hence lead to the determination of stellar rotation (Nielsen et al., 2013; Reinhold et al., 2013; McQuillan et al., 2014). Periodic variations of starspots due to activity cycles can also be revealed via light curve analysis (Reinhold et al., 2017; Arkhypov et al., 2015). However, space mission data allow only short-term cycles to be detected due to the relatively short observation intervals compared to Mount Wilson data. Mathur et al. (2014) studied the activity of 22 F-type stars and reported that only two of them showed 1400- and 650-day hints of activity cycles. Ferreira Lopes et al. (2015) analysed the CoRoT main sequence FGK-type stars and found stellar cycles ranging from 33 to 650 days.

Some Kepler and CoRoT Sun-like stars show short-term variations that are probably similar to the solar Rieger cycles (Lanza, 2010). The Rieger-type cycle ($P_{\rm R}$) is six to seven times longer than the rotation period of the Sun ($P_{\rm rot}$ is $\approx$ 26 days and the Rieger type periodicity is around 150-180 days). Lanza et al. (2009) studied the star CoRoT-2, which has a rotation period of 4.52 days and showed an additional periodicity of 29 days in its light curve, which may be analogous to the Rieger cycle. Bonomo & Lanza (2012) found a periodicity of 48 days in the light curves of the star Kepler-17 with $P_{\rm rot}$=12 days, which could also correspond to the Rieger period. Recently, Lanza et al. (2019) re-analysed the light curves of the same star for all Kepler quarters and found an additional cycle of 400-500 days. Arkhypov and Khodachenko (2021) studied 1726 Kepler stars and found two types of Rieger cycles: one independent of the stellar $P_{\rm rot}$ (for the stars with $T_{\rm eff} \lesssim$ 5500K) and the other proportional to $P_{\rm rot}$ (for the stars with $T_{\rm eff} \gtrsim$ 6300K). Therefore, it is becoming increasingly clear that space mission data may reveal Rieger cycles in the activity of other solar-like stars.

The Sun is a slowly rotating star with an equatorial period of around 26 days. Observations show that young solar-type stars rotate much faster than the present Sun. As a consequence, young solar-type stars may have vigorous magnetic dynamos and consequently strong magnetic activity. The young stars lose angular momentum via magnetised stellar winds (Mestel et al., 1968), and therefore their rotation slows down with age (Skumanich, 1972). As a response to slower rotation, the stellar dynamo also weakens with time, causing stellar activity to undergo a significant decrease (Ribas et al., 2005; Lammer et al., 2012). The stellar differential rotation may also change during the stellar evolution (Metcalfe and van Saders, 2017). With the recent Kepler mission, the rotation rate of thousands of stars was estimated (Nielsen et al., 2013; Reinhold et al., 2013; McQuillan et al., 2014).

Recently, Gurgenashvili et al. (2021) analysed the total irradiance of the Sun as a star to detect the Rieger-type periodicity. These authors found a clear signature of Rieger cycles, which was used to estimate the magnetic field strength in the dynamo layer. Inspired by the results of that work, we analyse the light curves of Kepler star KIC 2852336 to search for Rieger periodicity and attempt to probe the dynamo magnetic field in the stellar interior. Due to some restrictions, detecting a star with noticeable different periods other than the $P_{\rm rot}$ is quite challenging in Kepler data. Most frequently, only rotation periods are observed in Kepler periodograms. The longer periods need to be rigorously checked as, for the most part, they might be false, instrumental, or affected by multiple events and may not belong to stellar activity.

Data and methods

Several catalogues have been created from long-term Kepler data using automated methods. Nielsen et al. (2013) searched for rotation periods in more than 150 000 main sequence stars for Kepler quarters 2 to 9 (the online catalogue can be found at the CDS[10]). They found reliable $P_{\rm rot}$ values for 12,151 stars. Reinhold et al. (2013) analysed the light curves for 40 661 active Kepler stars from quarter 3 and found stable rotation periods between 0.5-45 days for 24 124 stars (the catalogue can also be found at the CDS[11]).

McQuillan et al. (2014) determined the rotation periods of more than 34 000 stars for quarters 3 to 14 and divided stellar populations into two different groups: fast-rotating young stars and slow-rotating old stars. The McQuillan catalogue[12] also includes 99 000 stars whose rotation periods could not be determined for various reasons. The Sun-like stars from this catalogue can be selected using different criteria. The first physical characteristic is the effective surface temperature, $T_{\rm eff}$ (5 778 K for the Sun). The second characteristic is the surface gravity, $\log g$ (which is 4.2

[10] http://cdsarc.u-strasbg.fr/viz-bin/qcat?J/A+A/557/L10

[11] http://cdsarc.u-strasbg.fr/viz-bin/qcat?J/A+A/560/A4

[12] https://vizier.u-strasbg.fr/viz-bin/VizieR?-source=J/ApJS/211/24

for the Sun). Therefore, the target stars should have similar values. The third characteristic is a rotation period, which varies between 0.5-70 days in this catalogue. To study the periodicity in the light curve of the star, we used a generalised Lomb-Scargle (GLS) periodogram, which is adequate for unevenly spaced data (Zechmeister & Kürster, 2009) and the wavelet transform (Torrence and Compo, 1998).

Table 4: Basic parameters of the star KIC 2852336 in the Kepler (rows 1 - 2), TESS (third row), and Gaia (last row) data archives. The metallicity and Kepler magnitude in the first row are taken from the Kepler archive. References: (1) McQuillan et al. (2014); (2) Mathur et al. (2017).

ID	$T_{\rm eff}$ (K)	$\log g$ cm/s^2	Parallax mas	$P_{\rm rot}$ (d)	Metallicity (Sun)	Radius ($R_{\rm Sun}$)	Mass ($M_{\rm Sun}$)	Mag
KIC 2852336 [1]	5 601	4.91	-	9.573	-0.229	0.571	0.9920	14.18
KIC 2852336 [2]	5 809	4.56	-	-	-0.26	0.837	0.930	-
TIC 137149729	5 723	4.41	-	-	-	1.043	1.02	13.66
Gaia DR2 2052578412798483072	5 480	-	1.3	-	-	1.11	-	14.13

There are two types of Kepler data: Simple Aperture Photometry (SAP) and Pre-search Data Conditioning (PDC) time series. SAP data are corrected only for the background flux and contain strong instrumental trends. Therefore, some additional corrections are needed to avoid systematics of instrumental origin. In PDC data, instrumental trends are mostly removed, and they are obtained after correction for the common trends shown by stars of similar magnitude and position on the same charge-coupled device (CCD) as the target. PDC data are sometimes strongly affected by the aggressive method used to correct for the instrumental trends, and all the variability on timescales longer than about 20-25 days is strongly reduced or suppressed, especially by the so-called multi-scale maximum a posteriori (msMAP) approach (Gilliland et al., 2015). So periods detected in the Kepler PDC data are probably very strong as they survived the correction process. Here we used the PDC data.

When the star moves from one CCD to another in the Kepler focal plane, the raw data display jumps from one quarter to the other, which can produce undesired effects in the computation of the GLS periodogram or Morlet wavelet. Therefore, we first had to remove these effects, which can be done by matching the median values between successive quarters. There are also gaps in the data of up to several days, and sometimes even several months, between the quarters, depending on the location of the stars on the Kepler focal plane. These gaps could be problematic during data analysis. The GLS works well with the unevenly spaced data; however, the Morlet wavelet needs evenly spaced data. One method to address this is to fill the gap with averages. We first calculated the daily averages and then filled the gaps using those averages.

We are interested in searching for the $P_{\rm R}$; therefore, we looked for periods of five to seven times the rotation period. Reliable oscillations in Kepler data can be found only with a period of < 90 days (one quarter in the Kepler time series). As such, we concentrated on stars with rotation periods of 5-15 days (younger analogues of the Sun).

Power spectra of Kepler stars normally show very pronounced peaks at the periods around $P_{\rm rot}$ and $P_{\rm rot}/2$. Longer periodicity is not usually seen unless one removes the peaks corresponding to stellar rotation. Finding a star with pronounced periods other than the $P_{\rm rot}$ is quite difficult in Kepler data. During the search for Sun-like stars with Rieger-type cycles in Kepler data, we found the star KIC 2852336, which showed pronounced periodicity near Rieger timescales. Therefore, we started to analyse the light curves of the star in detail. The star has $T_{\rm eff}$= 5 601 K and $\log g$ = 4.906 according to the McQuillan catalogue. Slightly different measurements can be found in Mathur et al. (2017) [13], with $T_{\rm eff}$ = 5 809, $\log g$ = 4.56, and [Fe/H] = -0.26. This star was also found in the Gaia archive (with ID Gaia DR2 2052578412798483072) [14] and TESS input catalogue (TIC 137149729) [15]. The basic parameters of the star are presented in Table 4.

Periods in Kepler data, which are longer than the rotation periods, need additional verification that they belong to stellar activity. First of all, one should exclude the existence of a companion star or the possibility of a multiple system. Kepler is limited to about 16 magnitudes and hence cannot detect stars that are much fainter. Our target star might have a fainter companion that stays beyond Kepler resolution. To exclude the influence of a faint companion or background star, we checked the Gaia data for stars in the vicinity of KIC 2852336. Gaia data contain stars that are

[13] https://vizier.u-strasbg.fr/viz-bin/VizieR?-source=J/ApJS/229/30

[14] https://gea.esac.esa.int/archive/

[15] https://archive.stsci.edu/missions-and-data/tess

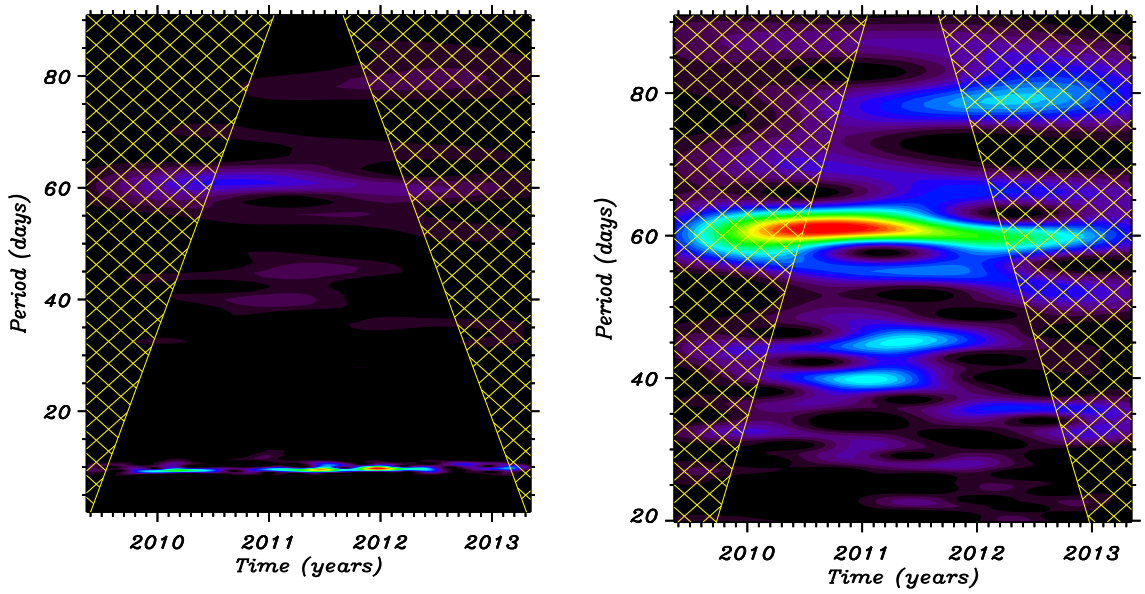

Figure 13: Morlet wavelet analysis of light curve variations during entire Kepler observations. The left panel shows the spectrum of the periods between 1-90 days, and the right panel shows the periods between 20-90 days ($P_{\rm rot}$ is removed). The hatched regions in the figure show the cone of influence, which means that the wavelet transform is not reliable in these areas.

5 mag fainter than the Kepler stars. We checked the Gaia archive using the same coordinates and could not find any companion within a radius of 11 arcsec, which indicates that this period is not caused by a companion star.

Rieger-type periodicity

The light curve of KIC2852336 (upper panel of Figure 12) shows a clear rotational modulation of around 9.5 days. The solid black line denotes the 20-day moving average, showing modulation of around 60-61 days. The lower panel of Figure 12 displays a significant peak at the period of 58-61 days, which corresponds to the timescale of Rieger-type periodicity. The Kepler data have been cleaned several times, eliminating instrumental effects or the effects of cosmic rays and the various types of noise, and therefore this period is probably not instrumental. However, it still needs to be carefully checked to verify that the period really characterises stellar activity.

Kepler data have some pronounced instrumental timescales, for example 30 and 90 days. For instance, every 30 days Kepler makes small adjustments to the spacecraft to send data to the ground by first re-pointing its radio antenna. Every 90 days (a time interval called a quarter in the Kepler jargon), the spacecraft (and therefore the focal plane) is rotated by 90 degrees. As the spacecraft rotates, a star jumps to another CCD with a different sensitivity and different settings than the previous one. The star returns to the same CCD in every fourth quarter. Therefore, if we see the same period in every fourth quarter only, we can assume that this period is instrumental (provoked by CCD settings) and therefore unreliable.

Figure 13 shows the Morlet wavelet spectrum of the light curve variations during the entire four years of Kepler observations. The rotation period is continuously seen during the whole interval, with more power in some quarters. The period of 61 days is also very well observed during all the observations. The right panel of the figure shows the power spectrum in the period interval of 20-90 days, which allows us to visualise the variation in this periodicity over time. The periodicity is seen in all quarters, which clearly shows that it is not CCD dependent.

We performed another analysis to prove that the periodicity is not instrumental. We chose a few stars that were located close to the target star, were similar to our target star in terms of magnitudes, effective temperatures, and surface gravity, and followed the same path across the Kepler CCDs. The Kepler space telescope is a Schmidt telescope composed of 21 Science CCD modules and four fine guidance sensor CCD modules. Each Science CCD module

consists of two 50x25 mm 2200x1024 pixel CCDs. Each Science module has four independent outputs and channels (for a total of 84 channels). We searched for these closest stars in all of the 17 quarters. The stars would be very close to our star if they fell on exactly the same CCD, same module, and same channel. If the other stars had the same periodicity in light curves, then the periodicity would be instrumental.

We found ten solar-type stars close to our star (see the stellar parameters in Table 5). Then we performed the GLS analysis of stellar light curves one by one. None of these stars had a peak around the period of 61 days. Figure 14 shows the GLS periodograms of four different stars from the above sample. This figure shows that the stars have very strong amplitudes at $P_{\rm rot}$, but any other periodicity is absent. Therefore, we are confident that the period of 58-61 days in the light curve of our target star is a real periodicity and corresponds to the Rieger cycle.

Besides the period of 60 days, GLS and wavelet analyses show another period near 40-45 days (see Figure 12 and Figure 13). The period has less power than the period of 58-61 days, but it is still seen on the power spectra. All the above analyses that ruled out instrumental effects are relevant to this period as well.

Solar Rieger-type periodicity is explained by magneto-Rossby waves in the dynamo layer, where the magnetic flux is periodically modulated by the waves and the quasi-periodic eruption of the flux towards the surface is triggered (Zaqarashvili et al., 2010, 2021). Then, due to the same mechanism, magneto-Rossby waves in the dynamo layer of our star may lead to the quasi-periodic modulation of magnetic structures on the stellar surface and therefore the modulation of the light curve.

In Figure 15, we plot the period versus dynamo magnetic field strength for magneto-Rossby wave modes with $m = 1$ and $n = 3, 4$ according to Eq. (43) from Gachechiladze et al. (2019), where m and n are the angular order and degree of spherical harmonics, respectively. We see that a dynamo magnetic field with a strength of 40 kG yields the observed periods of 61 days and 44 days for the harmonics of $n = 4$ and $n = 3$, respectively.

Table 5: Selected solar-type stars in the neighbourhood of our target star. $P_{\rm rot}$, $T_{\rm eff}$, and $\log g$ are taken from McQuillan et al. (2014).

KIC ID	RA (J2000)	Dec (J2000)	$T_{\rm eff}$ (K)	$\log g$ cm/s^2	$P_{\rm rot}$ (d)
2852336	19 25 41.066	+38 00 51.80	5 601	4.906	9.573
1570466	19 23 01.954	+37 08 35.99	5 715	4.302	8.637
1718985	19 23 41.969	+37 12 40.25	5 640	4.328	13.941
1723845	19 28 04.534	+37 12 20.05	5 521	4.446	9.373
1723978	19 28 12.530	+37 14 31.16	5 653	4.504	8.703
1870957	19 28 06.708	+37 22 31.04	5 765	4.332	6.608
2302942	19 25 46.339	+37 39 12.82	5 830	4.440	13.878
2011618	19 23 00.168	+37 28 06.28	5 564	4.534	11.876
2016657	19 27 44.402	+37 26 18.74	5 935	4.377	10.235
2443534	19 25 57.147	+37 42 58.18	5 863	4.504	10.723
2712799	19 25 31.961	+37 55 28.81	5 685	4.813	8.567

Discussion and conclusion

Detailed information about the Sun gathered over centuries can be used to study stellar atmospheres and interiors. On the other hand, recent space missions have collected a huge amount of information about many solar-like stars, though uncovering detailed processes in individual stars is not easy. Therefore, solar processes can be used to model the stellar atmosphere and interior, while solar-like stars at different stages of evolution can be used to study the time evolution of the Sun.

A Rieger-type periodicity of 155-180 day is an interesting observational feature seen in many indices of solar activity. The periodicity is probably connected with magneto-Rossby waves in the solar dynamo layer below the convection zone (Zaqarashvili et al., 2010, 2021). Therefore, observations and theoretical properties of the waves can be used to probe the layer, namely to estimate the dynamo field strength (Gurgenashvili et al., 2016, 2017; Zaqarashvili and Gurgenashvili, 2018). Total irradiance of the Sun is comparable to stellar light curves, and therefore it is important

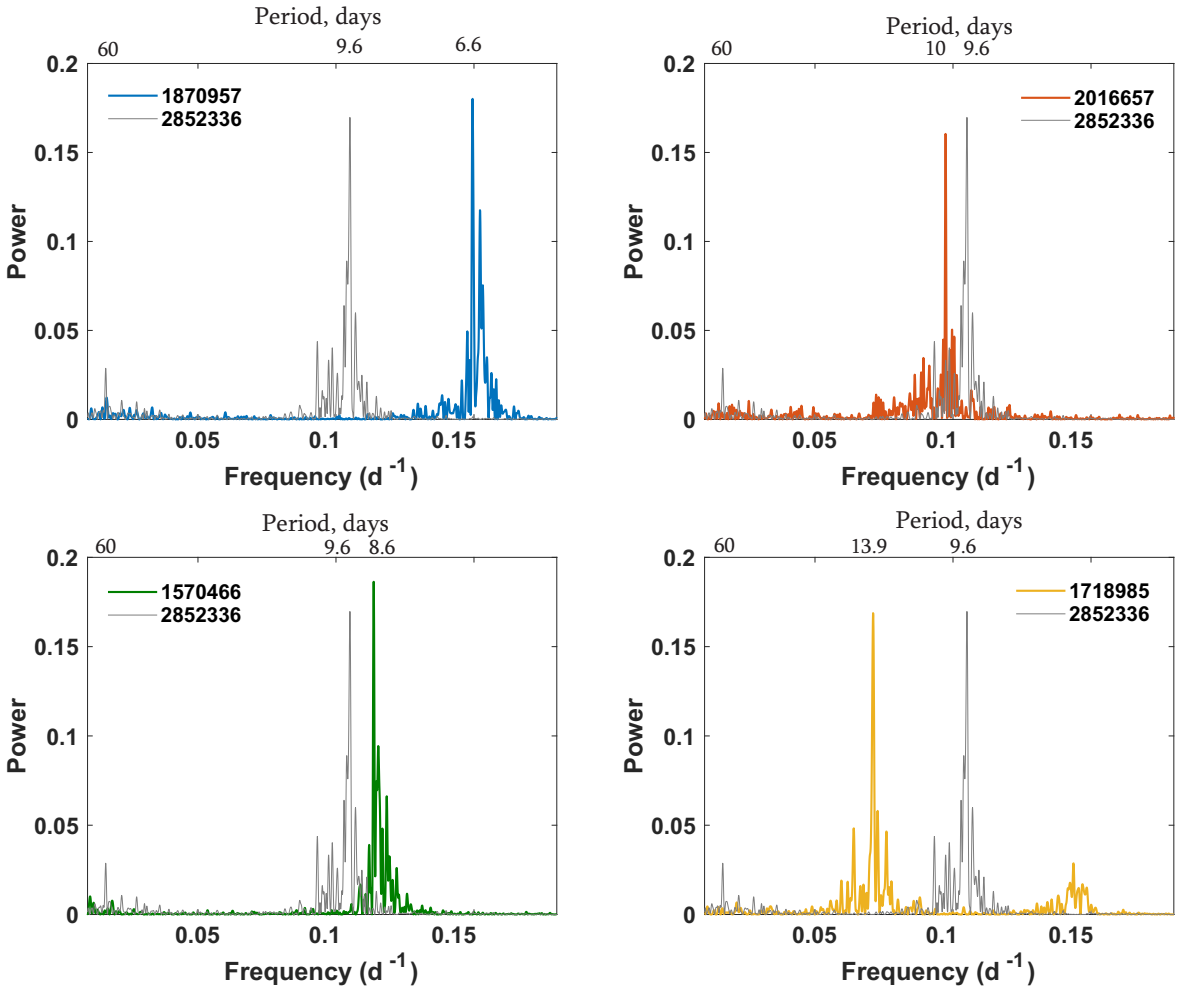

Figure 14: GLS periodograms of four Sun-like stars in the neighbourhood of the target star, marked with different colours. The thin grey line shows the periodogram of our target star for comparison.

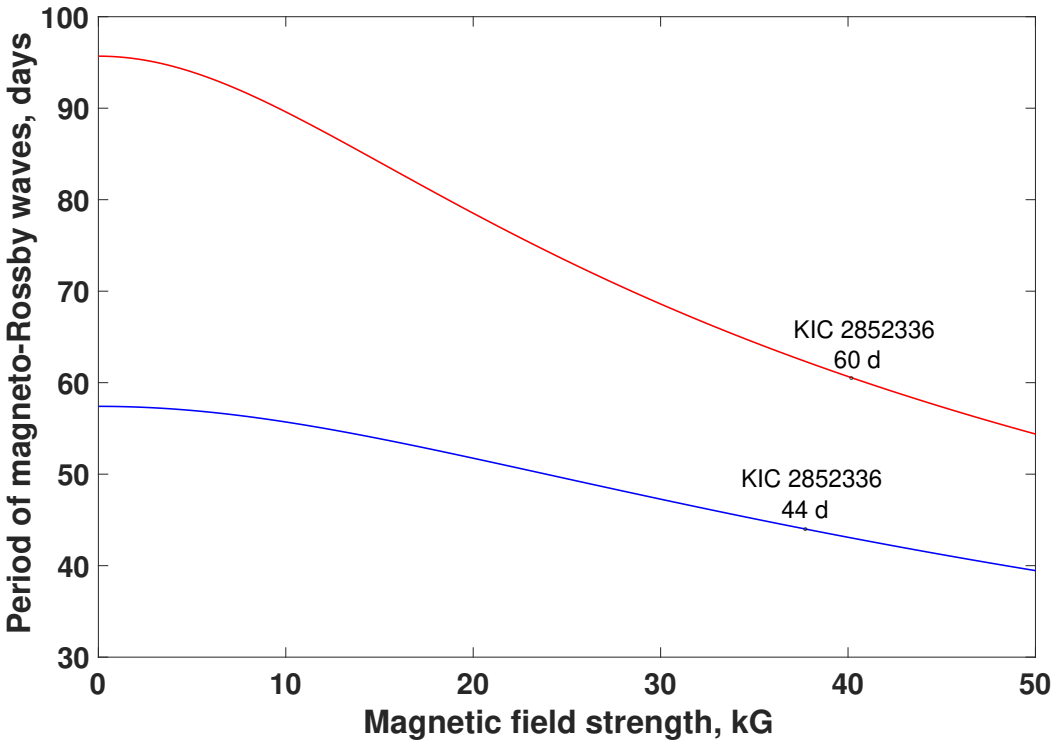

Figure 15: Period of magneto-Rossby waves vs. dynamo magnetic field strength. Here the red (blue) curve corresponds to the spherical harmonic with $m = 1$ and $n = 4$ ($n = 3$), where m and n are the angular order and degree.

to first look into Rieger-type periodicity in the irradiance. Gurgenashvili et al. (2021) studied the total solar irradiance during solar cycles 23 and 24 and found two distinct periods of 185 days and 115 days (in cycle 23) and 170 and 145 days (in cycle 24), which led to the estimation of the dynamo field strength as 10-15 kG. It is thus important to perform a similar analysis on solar-type stars and compare the results to those of the Sun.

We analysed the light curve of the Kepler star KIC 2852336 ($P_{\rm rot}$ = 9.5 days), which is a young analogue of the Sun. We found a very clear period of 58-61 days in the power spectrum of stellar light curve oscillations, which is the timescale of Rieger-type periodicity for the star. We used different methods to confirm that this periodicity is a real variation of stellar irradiance and not instrumental or from some other source. First, we checked for the existence of faint companion stars with the same coordinates in the Gaia archive but found that this star has no companion within a radius of 11 arcsec. Second, we checked whether the period is provoked by particular CCD settings (due to the spacecraft rotation, the star returns to the same CCD in every fourth quarter, i.e. every 90 days). However, the periodicity is seen during whole observations (Figure 13), and therefore CCD dependence is also ruled out. Third, we checked other stars with similar magnitudes, temperatures, and surface gravity from exactly the same CCD channel. Light curves of several stars did not display any indication of 58-61 day and 40-44 day periods, which confirmed that the periodicity in our target star really corresponds to its activity. There might be several reasons for the absence of clear Rieger cycles on those stars. First, stars might be tilted such that only polar regions are observed from the Earth. If spots (and structures associated with strong magnetic fields) appear near equatorial regions like on the Sun, then they will not affect the stellar light curve. Second, Kepler observations lasted only 4 years, a time span in which many stars do not complete an entire activity cycle. Rieger periodicity on the Sun appears only near activity maximum; therefore, if a star is in its minimum phase, then it will not show the Rieger periodicity. Third, Rieger-type cycles might exist in some stars but not be visible due to weak peaks in the power spectrum. Below we discuss several consequences of our analysis, which may become important points in stellar evolution.

One important aspect in stellar evolution is connected with the stellar magnetic field, which governs activity in the form of starspots, stellar flares, and coronal mass ejections. The magnetic field of solar-type stars is believed to be amplified in the dynamo layer below or inside the convection zone. The magnetic flux rises towards the surface owing

to the magnetic buoyancy and appears in the form of starspots. It is known that younger stars show faster rotation and the rotation period rate decreases with age (Skumanich, 1972; Lammer et al., 2012). One plausible mechanism for this slowdown is the magnetic breaking when the stellar wind flowing along the magnetic field lines takes the angular momentum from stars (Mestel et al., 1968). Therefore, magnetic field evolution throughout the main sequence is an important factor in stellar life. To understand the magnetic field evolution process, it is of vital importance to know the dynamo field strength at different stages of stellar evolution. The field strength in the stellar dynamo layer can be estimated via asteroseismology, but it is a difficult task. Therefore, even a rough estimation of the dynamo field strength in stellar interiors may become a key point in understanding stellar magnetic evolution.

The most plausible mechanism for Rieger-type periodicity is magneto-Rossby waves in the solar dynamo layer, which lead to the modulation of the dynamo field and consequently trigger the quasi-periodic eruption of magnetic flux towards the surface (Zaqarashvili et al., 2010). Therefore, the observed periods and dispersion relation of magneto-Rossby waves can be used to estimate the dynamo magnetic field strength (Gurgenashvili et al., 2016, 2017; Zaqarashvili and Gurgenashvili, 2018). Gurgenashvili et al. (2021) analysed the total solar irradiance data for solar cycles 23 and 24 and found the existence of periods of 185 and 115 days and 170 and 145 days, respectively, which were explained as being due to the spherical harmonics of magneto-Rossby waves with $m = 1$ and $n = 4, 3$. Consequently, a magnetic field of $\sim$ 10-15 kG was estimated in the solar dynamo layer. The periods in the light curve of the target star are found to be around 58-61 days and 40-44 days, which satisfy the same ratio of $P_R/P_{\rm rot}$ as for the Sun. Figure 15 shows that a dynamo field strength of 40 kG yields the observed periods for the magneto-Rossby wave harmonics with $m = 1$ and $n = 4, 3$. Therefore, the estimated dynamo field in our target star is three times stronger than that of the Sun estimated with the same method (Gurgenashvili et al., 2021). The rotation period of the target star (9.5 days) is also three times smaller than the rotation period of the Sun (27 days). Therefore, a comparison of the rotation periods and estimated dynamo magnetic field strengths of our star and the Sun shows an interesting ratio,

$$\frac{\Omega_{star}}{\Omega_{Sun}} \sim \frac{B_{star}}{B_{Sun}} \approx 3, \tag{3}$$

which can be rewritten as

$$\frac{\Omega}{B_D} \approx const, \tag{4}$$

where Ω is the stellar angular velocity and B_D is the dynamo magnetic field strength. Equation (2) shows that the dynamo magnetic field is proportional to the rotation during stellar evolution, and therefore young fast-rotating solar-type stars should show a stronger field and hence stronger magnetic activity. This has long been known, and therefore our result agrees with other observations (for a theoretical discussion, see e.g. Durney & Robinson (1982)). The advantage of Eq. (3) is that one can estimate the dynamo field from the stellar rotation period. However, Eq. (3) is obtained from the analyses of the Sun and one other star and could therefore be just coincidence. More stellar samples are required to confirm it.

4 Thesis discussion and conclusion

Rieger periodicity has been detected in various activity indices of the Sun for several decades. It is often referred to have enigmatic properties as it does not consistently characterize solar cycles and its period changes from cycle to cycle. There are many works about the Rieger periodicity on the Sun including its disappearance/appearance (Carbonell & Ballester, 1990; Carbonell and Ballester, 1992; Lean, 1990). Recent studies have shown that the Rieger periodicity is characterized by a certain regularity, which is manifested by anti-correlation of its period with solar cycle strength. Long-period records of solar cycles showed that the period becomes shorter in stronger cycles and vice versa (Gurgenashvili et al., 2016). It is known that solar activity is asymmetric with regards to the hemispheres, which means that one hemisphere normally is more active than the other. Solar activity generally shows north-south asymmetry in many indicators (Spörer , 1894; Maunder , 1904; Carbonell et al., 1993; Oliver and Ballester, 1994; Ballester et al., 2005; Temmer et al. , 2002, 2006). It was found that the Rieger periodicity also reflects this asymmetry i.e. the stronger hemisphere showed the shorter period than the weaker one in individual cycles (Gurgenashvili et al., 2017).

Observed correlation between the Rieger cycle length and solar activity strength suggests that the periodicity is related to the dynamo layer in the solar interior. Various mechanisms were proposed to explain the mechanism of the Rieger periodicity, but the most successful explanation is related to Rossby-type waves in the solar tachocline. Zaqarashvili et al. (2010) showed that the dynamo magnetic field and the latitudinal differential rotation in the tachocline below the solar convective layer cause the instability of magnetic Rossby waves, which may provoke the quasi-periodic eruption of magnetic flux towards the solar surface. Since the period of magnetic Rossby waves depends on the magnetic field strength, the observed periodicity should be related to the level of solar magnetic activity. This was successfully demonstrated by observations (Gurgenashvili et al., 2016). Therefore, the theoretical dispersion relation of magnetic Rossby waves and the observed Rieger periods in solar activity make it possible to estimate the strength of the dynamo magnetic field in the solar interior. This method may also be used for other solar-type stars.

The main goal of the thesis was to study short-term variations in the light curves of Sun-like stars, which are probably caused by their magnetic activity. As the short-term cycles are well studied on the Sun, it was essential to look into the Sun as a star variations before starting to search for the stellar cycles. Stellar light curves obtained by space missions are analogous to the total solar irradiance (TSI). Therefore, the goal was to study the Rieger periodicity in TSI. TSI is influenced by the global solar magnetic field which includes sunspot darkening and faculae brightening. Sunspots are usually concentrated near the equator, while the faculae are mostly distributed in higher latitudes.

While the Sun is studied in details for long time, the information about distribution of spots and faculae on other solar-type stars is not well known. Other stars may require different models due to different ratios of spots and faculae, so the solar model should be used with caution on other stars. Recent Kepler and CoRoT space missions collected huge amount of data about stellar activity, which gives an excellent basis to search for the Sun-like periodicity on other stars. Then the observed periodicity on stars with different rotation rate will be very important to understand the variation of dynamo activity along stellar evolution.

The first mission of Kepler provided continuous, high-precision photometry of hundreds of thousand stars over four years. The stellar radiation flux significantly depends on the presence of active regions on their surfaces, therefore it is presumably changing due to appearance of star spots. Most of the Kepler observations are about Sun-like stars. Therefore, there is a large database for studying the solar analogs, which gives us an excellent opportunity to look for the solar Rieger-type periods on other stars. However, pure understanding of stellar activity and short observation

intervals make it difficult to detect short-period cycles. Very little is known about short periodic cycles from ground-based observations. The most significant example here is τ Bootis (Baliunas et al., 1995; Mittag et al., 2017; Mengel et al., 2016), which has been studied by various authors. Furthermore, there is a significant limitation in the time range of data from space missions, which makes even more challenging to find activity cycles. For example, four year observation interval of Kepler is not long enough to observe complete stellar cycles. Moreover, the phase of stellar activity is very important. According to solar observations, the Rieger periodicity appears only near activity maxima, therefore to find the similar cycles on stars being in minimum of their activity is nearly impossible. As Kepler stars are mostly young Suns, the rotation modulation is the strongest in their light curves, therefore the rotation period is the only thing that can be found in most of the stars. On the other hand, it is also very hard to observe the short activity cycles on stars those axes of rotation are nearly parallel to the line of sight.

The magnetic variability of Sun-like stars has been monitoring for a long time since Wilson (1978) and Baliunas et al. (1995). After the nearly four-year space odyssey of Kepler's first mission, it became possible to process data from hundreds of thousands of stars using various methods (Mathur et al., 2014; Vida et al., 2014). Short cycles can be found in the activity of some Kepler stars (Bonomo & Lanza, 2012; Lanza et al., 2019), as well as in CoRoT stars (Ferreira Lopes et al., 2015), which perhaps correspond to the Rieger periodicity of the Sun.

The current thesis is based on two refereed papers. The first paper deals with the study of TSI in solar cycles 23-24. We used SOHO/VIRGO TSI observational data which covers the last two cycles. We also used SATIRE-S reconstructed data for comparison. Since the main contributors to TSI are sunspots and faculae, we studied both components separately in both cycles. Additionally, we used sunspot area data (both full-disk daily records and hemispheric data) for comparison. The main results are:

Cycle 23: The Morlet wavelet analysis of TSI showed two periods of 180 and 115 days. The period of 180 days is also clearly seen in the sunspot data of the northern hemisphere, but it is absent in faculae data. Therefore, the 180 days cycle is probably related to sunspots, where the strong magnetic field is concentrated, but not to faculae, where the magnetic field is relatively weaker. It agrees with previous studies that the Rieger periodicity is associated only with strong magnetic flux.

The 115-day periodicity is seen also in the sunspot data and it is probably associated with the southern hemisphere.

Cycle 24: Wavelet analysis of TSI showed strong evidence of 170-day and 145-day periodicity, while only 190 and 145-day periods were visible in sunspot data. Note that the 190-day period did not appear in TSI (the period is probably cancelled in TSI due to the opposite effects of sunspot and faculae contributions).

There is an evidence that TSI is influenced mainly by sunspots rather than faculae, so understanding their individual contributions is crucial. Some oscillation period was only visible in sunspot or faculae data, but not in TSI. Cross-wavelet analysis showed that the 165-day and 140-day periods in solar cycle 23 are only seen in the GRO sunspot area data, not in the TSI. It was found that both faculae and sunspots showed the 140-day periodicity. Their amplitudes were similar, but the oscillations were in antiphase. Therefore, the contributions of the periods in TSI cancel each other. The 115-day period, which is visible both in spots and faculae, has a significant contribution to the TSI. Nevertheless, oscillation signals in the two data become stronger at different times, which increases the contribution of the period in TSI. The 190-day period continuously appear during the cycle 24 in spot and faculae data, but their contributions cancel each other ant the period does not appear in TSI.

In the second paper, we searched the short-term Rieger cycles in solar-type stars. Most of Kepler stars are young solar analogues, which are quite different from each other. In general, activity cycles of young stars are more irregular than that of solar-age stars. Instead, the rotation period is more pronounced in young stars. After looking to the light curves of thousands of Kepler stars, we concluded that to find periods longer than the rotation ones is challenging task. The vast majority of these stars only show rotation periods and their half periods. On the other hand, existed longer periods in stellar power spectra could be instrumental. Moreover, due to the peculiarities of the Kepler observations, the periods above 90 days are unreliable. Therefore, the analysis is limited to the periods of < 90 days. Consequently, to find the short term cycles in Kepler data requires extra caution and double-checking. Furthermore, as the Kepler magnitude is limited to 16, the fainter companion stars can not be detected, but they may cause the observed periods in light curves. To exclude this possibility, one check Gaia data, which perceives fainter stars.

Another peculiarity of the Kepler spacecraft is that it rotates with 90 degrees every 90 days, which causes to shift stars over the CCD. As a result, the delay between the Kepler quarters could be 3-4 days or more, hence the data are unevenly distributed. Therefore, we used GLS method to analyse such unevenly distributed data. We also used the wavelet analysis of daily averaged data, which is a helpful tool to see a localized period in time.

We found an interesting solar-like star KIC 2852336 with a rotation period of about 9.5 days. The light curve of the star showed pronounced period of 61 day and less pronounced peak at 40-44 days. We checked the stellar data

by several ways. First, we searched the possible presence of a faint companion in the Gaia data. Then we looked for the existence of the period in specific quarters to exclude its appearance due to CCD peculiarities. We also studied the light curves of 10 nearby stars to find a similar period (which would be a sign of a CCD peculiarities). After all these studies, it was found that this star did not have any companion that could affect the light curve. This periodicity appeared continuously and did not depend on Kepler quarters. None of the stars in its close neighbourhood showed a period different from the rotation period. Therefore, we concluded that the periodicity on this star was real and it was connected to the variation of its magnetic activity.

Next we used the dispersion relation of magnetic Rossby waves and the periods detected on the Sun and the star KIC 2852336 to estimate the magnetic field strengths in the solar and stellar dynamo layers. Magnetic field strength in stellar dynamo layers is crucial to understand which dynamo model is responsible for stellar activity. However, direct measurement of the magnetic field in solar/stellar interiors is impossible; therefore invoking of indirect methods is necessary to make estimations. As the Rieger periodicity probably corresponds to magnetic Rossby waves in dynamo layers, the observed periods can be used to probe the internal magnetic fields. Then the observed and the theoretical periods will tell us about the strength of dynamo magnetic field in solar-like stars at different phases of evolution. Eq. 43 of Gachechiladze et al. (2019) was used to calculate the relationship between the dynamo magnetic field strength and the period of magnetic Rossby waves. According to the equation, the 180 and 125-day periods in TSI were found to correspond to different harmonics of Rossby waves in the case of 12 kG magnetic field. The same equation results in 40 kG magnetic field using the observed 60 and 44-day periods in our star. Hence, the stellar dynamo magnetic field was found to be almost three times stronger than the solar counterpart. Interestingly, the solar rotation period is also about three times longer than that of KIC 2852336. Therefore, the ratio of angular velocity and magnetic field strength was found to be the same for the Sun and KIC 2852336. It is an interesting question whether it is occasional or typical for Sun-like stars. It is not possible to make any conclusion based on the example of one star. Therefore, it requires to have more examples of Sun-like stars.

Several open questions remain after the thesis. Are the Rieger cycles unique features of this star? Do other stars have similar periodicity? The ratios between the Rieger and the rotation periods are about 6.4 and 6.6 for the Kepler star KIC 2852336 and the Sun, respectively. So a question is: what is the ratio for other stars? The relationship between the rotation periods and the magnetic fields of the Sun and the star KIC 2852336 opens further question: will the coefficient be again 3 for other stars? These questions naturally suggests the future studies.

We scored 34030 stars in the McQuillan catalog and restricted by temperature, surface gravitation and period of 5-15 days to separate young Sun-like stars (stars rotating faster than 5 days do not have regular cycles, and for the slower-rotating stars, the Rieger period can be relatively less accurate). The restriction led to 3629 stars. Then we used the GLS analysis for each star to find the potential Rieger period. The preliminary result was that 2901 stars (about 80%) showed only rotation periods, but not Rieger cycles. 728 stars (about 20%) displayed the possible short term cycles. We considered only the periods longer than $2P_{\rm rot}$ to exclude peaks associated with $P_{\rm rot}$. 26 from these stars had only 90-day period, which is probably instrumental (due to the rotation of the satellite). These stars represent 0.7% of the total stars and must excluded from further analysis. Hence, 702 stars remain with potential Rieger cycles. We plan to study the light curves of these stars to have a wider picture of the cycles in stars with different evolutionary phases.

Aknowledgement

First, I would like to thank my supervisors, Teimuraz Zaqarashvili and Ansgar Reiners, for their outstanding contributions to my research. As both professors are very busy all the time, they always found time for my problems. Teimuraz, a special thank you because you have always been like a father and a friend to me over the years, not just a super supportive supervisor. Ansgar, thank you for creating the best working environment because I always felt at home in the university and the group. Thank you so much for always being super helpful and always ready to solve any problem or issue I had.

I am very grateful to Vasil Kukhianidze, because without him it would have been very difficult for me to study new and complex issues and analyze Kepler data. Thank you for the friendship and your support, for always being by my side and making me feel confident all these years. Thanks to Timo Reinhold for his friendship, support and always helpful comments that significantly improved both papers.

Thanks to our co-authors Ramon Oliver and Antonino F. Lanza, without whose exciting comments and discussions, my research would not be what it is today. Thanks to Jens Niemeyer, for the support and attending all of my progress report. Thanks to the program coordinators, Aleksandra Bovt and Vakhtang Pataridze.

Thanks to my friends who have put up with my nagging and endured hardships with me over the years. Thanks to Mariam Albekioni, without whom I can't imagine the last and the following years, for always being by my side, encouraging and supporting me. Thanks to Anina Timmerman for the good friendship. I will always miss the common complaints with you. Thanks to all my friends who kept telling me that I am a good scientist when I doubted it.

Finally, many thanks to my family, my mother, who really wanted to attend the day I became a doctor, and my father, who was always proud of me.

References

Akimov, L. A., & Belkina, I. L. 2012, SoSyR, 46, 243

Arkhypov, O. V., Khodachenko, M. L., Lammer, H., Güdel, M., Lüftinger, Th., Johnstone, C. P., 2015, ApJ, 807, 109

Arkhypov, O. V. & Khodachenko, M. L., 2021, A&A, 651,A28

Bai, T., & Cliver, E. H. 1990, ApJ, 363, 299

Bai, T., & Sturrock, P. A., 1987, Nature, 327, 601

Bai, T., & Sturrock, P. A. 1991, Nature, 350, 141

Ballester, J. L., Oliver, R., & Carbonell, M. 2002, ApJ, 566, 505

Ballester, J. L., Oliver, R., & Baudin, F. 1999, ApJL, 522, L153

Ballester,J.L., Oliver, R., Carbonell, M., 2004, ApJ, 615(2), 173.

Ballester, J. L., Oliver, R., & Carbonell, M. 2005, A& A, 431, L5

Bogart, R. S., & Bai, T. 1985, ApJL, 299, L51

Baglin, A., Auvergne, M., Barge, P., Deleuil, M., & Michel, E., 2008, Proceedings of the International Astronomical Union, 4(S253), 71-81

Baliunas, S. L., Donahue, R. A., Soon, W. H., et al. 1995, ApJ, 438, 269

Baliunas, S. L., Nesme-Ribes, E., Sokoloff, D., & Soon, W. H. 1996, ApJ, 460, 848

Baliunas, S. L., Henry, G. W., Donahue, R. A., Fekel, F. C., & Soon, W. H. 1997, ApJ, 474, L119

Baliunas, S. L., Donahue, R. A., Soon, W. H., & Henry, G. W. 1997, in ASP Conf. Sere Vol. 154, Cool Stars, Stellar Systems, and the Sun, 10th Cambridge Workshop, ed. R. Donahue & J. Bookbinder (San Francisco: ASP),153

Böhm-Vitense, E. 2007, ApJ, 657, 486

Bonomo, A. S., & Lanza, A. F. 2012, A&A, 547, A37

Borucki, W., Koch, D., Basri, G., Batalha, N. et al., 2010, Science, 327, 5968, 977

Brandenburg,A., Saar,S.H.,& Turpin,C.J. 1998, ApJ,498,L51

Carbonell, M., & Ballester, J. L. 1990, A&A, 238, 377

Carbonell, M., & Ballester, J. L. 1992, A&A, 255, 350

Carbonell, M., Oliver, R., & Ballester, J. L. 1993, A&A, 274, 497

Chapman, G. A., Cookson, A. M., & Dobias, J. J., 1997, ApJ, 482, 1

Charbonneau, P., 2010, LRSP, 7, URL : http://www.livingreviews.org/lrsp-2010-3

Dasi-Espuig, M., Jiang, J., Krivova, N. A. et al. 2016, A&A, 590, A63

Dennis, B. R. 1985, SoPh, 100, 465

do Nascimento, Jr., J.-D., Saar, S. H., & Anthony, F. 2015, in 18th Cambridge Workshop on Cool Stars, Stellar Systems, and the Sun, eds. G. T. van Belle, & H. C. Harris, Cambridge Workshop on Cool Stars, Stellar Systems, and the Sun, 18, 59

Dimitropoulou, M., Moussas, X., & Strintzi, D. 2008, MNRAS, 386, 2278

Dröge, W., Gibbs, K., Grunsfeld, J. M., Meyer, P., Newport, B. J., Evenson, P., & Moses, D. 1990, ApJS, 73, 279

Delache Ph., Laclare F., & Sadsoud H. 1985, Nature, 317,416

Distefano,E., Lanzafame,A.C., Lanza,A.F., Messina,S., Spada, F., 2017, A&A, 606, 58.

Durney, B.R. & Robinson, R. D., 1982, ApJ, 253, 290

Ferreira Lopes,C.E., Le ao,I.C., de Freitas, D.B., Canto Martins,B.L., Catelan,M., De Medeiros, J.R. 2015 A&A., 583, 134

Fröhlich, C., Romero, J., Roth, H. et al. 1995, Sol. Phys., 162, 101

Gachechiladze, T., Zaqarashvili, T. V., Gurgenashvili, E., Ramishvili, G., Carbonell, M., Oliver, R., Ballester, J.L., 2019, ApJ, 874,162

García, R. A., Mathur, S., Salabert, D., et al. 2010, Science, 329, 1032

Gleissberg, M. N. 1939, Obs, 62, 158

Gurgenashvili, E., Zaqarashvili, T. V., Kukhianidze, V., Oliver, R., Ballester, J. L., Ramishvili, G., Shergelashvili, B., Hanslmeier, A., Poedts, S., 2016, ApJ, 826, 55

Gurgenashvili, E., Zaqarashvili, T. V., Kukhianidze, V., Oliver, R., Ballester, J. L., Dikpati, M., McIntosh, S.W., 2017, ApJ, 845, 137

Gurgenashvili, E., Zaqarashvili, T. V., Kukhianidze, V., Reiners, A., Oliver, R., Lanza, A. F. & Reinhold, T., 2021, A&A, 653, A146

Gilliland, R. L., Chaplin, W. J., Jenkins, J. M., Ramsey, L. W., & Smith, J. C. 2015, AJ, 150, 133

Ichimoto, K., Kubota, J., Suzuki, M., Tohmura, I., & Kurokawa, H. 1985, Nature, 316, 422

Hathaway, D. H. 2010, LRSP, 7, 1, URL: http://solarphysics.livingreviews.org/Articles/lrsp-2010-1

Hoyt, D.V., Kyle, H.L., Hickey, J.R., Maschhoff, R.H., 1992, J Geophys Res 97:51–63

Hanslmeier, A., Brajša, R., Čalogović, J., et al. 2013, A&A, 550, A6

Hide, R., 1966, Philos. Trans. R. Soc. Lond. Ser. A 259, 615

Kile, J. N., & Cliver, E. W. 1991, ApJ, 370, 442

Kiplinger,A.L., Dennis,B.R., Orwig, L.E., 1984, Bulletin of the American Astronomical Society,16,891

Kopp, G., Lawrence, G., Rottman, G., 2005, Sol Phys 230,129.

Krivova, N. A., & Solanki, S. 2002, A&A, 394, 701

Krivova, N. A., Solanki, S. K., Wenzler, T. and Podlipnik,B. 2009, JGRA, 114, D1.

Krivova, N. A., Vieira, L. E. A. and Solanki, S. K. 2010, JGR, 115, A12112

Lanza, A. F., Pagano, I., Leto, G., et al. 2009, A&A, 493, 193

Lanza,A.F., Netto, Y., Bonomo,A.S., Parviainen, H., Valio,A., Aigrain, S., 2019, A&A, 626, 38

Lanza, A. F. 2010, in IAU Symp. 264, eds. A. G. Kosovichev, A. H. Andrei, & J.-P. Roelot, 120

Lou, Y.Q. 2000, ApJ, 540, 1102

Lobzin,V. V., Cairns, I. H., & Robinson, P. A. 2012, ApJL, 754, L28

Lammer, H., Güdel, M., Kulikov, Y., et al. 2012, Earth Planets Space, 64, 179

Lean, J. L., & Brueckner, G. E. 1989, ApJ, 337, 568

Lean, J. L. 1990, ApJ, 363, 718

Lee, R.B., 1987, Appl Opt 26:3090–3096

Lockwood, G. W., Skiff, B. A., Henry, G. W., et al. 2007, ApJS, 171, 260

Löptien, B., Gizon, L., Birch, A. C., et al. 2018, NatAs, 2, 568

Markwardt, C. B. 2009, in Astronomical Society of the Pacific Conference Series, Vol. 411, Astronomical Data Analysis Software and Systems XVIII, ed. D. A. Bohlender, D. Durand, & P. Dowler, 251.

Massi,M., Neidhöfer,J., Carpentier,Y., Ros,E., 2005, A&A,435, 1

Moré, J. J. 1978, The Levenberg-Marquardt algorithm:Implementation and theory, Springer, 630, 105

Messina, S., & Guinan, E. F. 2002, A&A, 393, 225

Montet,B.T., Tovar, G., Foreman-Mackey, D., ApJ, 851, 116

Mathur, S., Huber, D., Batalha, N. M., et al. 2017, ApJS, 229, 30

Mathur,S., García, R.A., Ballot,J., Ceillier,T., Salabert,D., Metcalfe,T.S., Régulo,C., Jímenez,A., Bloemen,S.,2014, A&A, 562, 124

McIntosh, S. W., Leamon, R. J., Krista, L. D., et al. 2015, Nature Communications, 6, 6491

McIntosh, S. W., Cramer W. J., Marcano M. P., and Leamon, R. J., 2017, Nature Astronomy, 1, 0086

McQuillan A., Mazeh T., Aigrain S., 2014, ApJS, 211, 24

Mittag, M., Robrade, J., Schmitt, J. H. M. M., et al. 2017, A&A, 600, A119

Mittag,M., Schmitt,J.H.M.M., Hempelmann,A., Schroeder,K.-P., 2019, A&A, 621, 136

Mengel, M. W., Fares, R., Marsden, S. C., et al. 2016, MNRAS, 459, 4325

Mestel, L. 1968, MNRAS, 138, 359

Metcalfe, T. S. and van Saders, J., 2017, Sol. Phys., 292, 126

Maunder, E.W., 1904, MNRAS., 64, 747

Nielsen M. B., Gizon L., Schunker H., Karoff C., 2013, A&A, 557, L10

Noyes, R. W., Weiss, N. O., and Vaughan, A. H. 1984, ApJ, 287, 769

Nèmec, N. E., Shapiro, A. I., Krivova, N. A., et al. 2020, A&A, 636, A43

Oláh, K., & Strassmeier, K. G. 2002, Astron. Nachr., 323, 361

Oláh, K., Kolláth, Z., & Strassmeier, K. G. 2000, A&A, 356, 643

Oláh, K., Kolláth, Z., Granzer, T., et al. 2009, A&A, 501, 703

Oliver, R., & Ballester, J. L. 1994, SoPh, 152, 481

Oliver, R., Ballester, J. L., & Boudin, F. 1998, Nature, 394, 552

Ozguc, A., Atac, T., 1989, SoPh, 123(2), 357

Parker, E. N., 1958, ApJ, 128, 677P

Pap,J., Tobiska, W.K., & Bouwer, S.D., 1990, SoPh, 129(1), 165

Radick, R.R., Lockwood, G. W., & Baliunas, S.L., 1990, Science, 247, 4938

Radick R.R., Lockwood G.W., Skiff B.A., Baliunas S.L., 1998, ApJS, 118, 239

Ribas, I., Guinan, E. F. Güdel, M., & Audard, M., 2005, ApJ, 622, 680

Ricker, G. R., Winn, J. N., Vanderspek, R., et al. 2014, in Society of Photo-Optical Instrumentation Engineers (SPIE) Conference Series, Vol. 9143, Proc. SPIE, 914320

Rieger, E., Share, G. H., Forrest, D. J., Kanbach, G., Reppin, C., et al. 1984, Nature, 312, 623

Ribes,E., Merlin,P., Ribes, J.-C., Barthalot,R., 1989, Ann. Geophys. 7, 321

Reinhold T., Reiners A., Basri G., 2013, A&A, 560, A4.

Reinhold, T., Cameron, R. H., & Gizon, L. 2017, A&A, 603, A52

Reinhold, T., Bell, K. J., Kuszlewicz, J., Hekker, S., Shapiro, A.I., 2019, A&A, 621, A21

Rossby, C.-G., 1939, J. Mar. Res. 2, 38

Rossby, C.-G., 1945, J. Atmos. Sci. 2, 187

Saar, S. H., & Brandenburg, A. 1999, ApJ, 524, 295

Salabert, D., Régulo, C., García, R. A., et al. 2016, A&A, 589, A118

Skumanich, A. 1972, ApJ, 171, 565

Schatten, K. H. 1993, JGR, 98, 18

Schmitt,J.H.M.M. & Mittag,M., 2017, A&A, 600, 120

Schwabe H., 1844, Astronomische Nachrichten, 21, 233

Silverman, S.M., 1990, Nature, 347, 365.

Solanki, S. K., Usoskin, I. G., Kromer, B., Schüssler, M., & Beer, J. 2004, Natur, 431, 1084

Sturrock, P. A., Bertello, L., Fischbach, E., Javorsek, D., Jenkins, J. H., et al. 2013, APh, 42, 62

Sturrock, P. A., Bush, R., Gough, D. O., & Scargle, J. D. 2015, ApJ, 804, 47

Spörer, G., 1894, ibid Nr., 32, 10

Temmer, M., Veronig, A., & Hanslmeier, A. 2002, A&A, 390, 707

Temmer, M., Rybák, J., Bendík, P., Veronig, A., Vogler, F., Otruba, W., Pötzi, W., Hanslmeier, A., 2006, A&A., 447, 735.

Torrence, C. & Compo, G. P., 1998, BAMS, 79, 61

Usoskin, I. G., Solanki, S. K., & Kovaltsov, G. A. 2007, A&A, 471, 301

Vaquero, J.M., Trigo, R.M., Vázquez,M., Gallego,M.C.,2010, New Astron. 15(4), 385

Vaughan, A. H., & Preston, G. W. 1980, PASP, 92, 385

Vecchio, A., & Carbone, V. 2009, A&A, 502, 981

Verma, V. K., Joshi, G. C., Uddin, W., & Paliwal, D. C. 1991, A&A, 90, 83

Vida, K., Olah, K., & Szabo, R. 2014, MNRAS, 441, 2744

Wilson, O. C. 1968, ApJ, 153, 221

Wilson, O. C. 1978, ApJ, 226, 379

Willson, R.C., 1984, Space Sci Rev, 38:203–242

Willson, R.C., 1994,IAU Colloquium No. 143, Cambridge University Press, Cambridge, pp 54–62

Willson, R.C., 2001, Earth Observer 13:14–17

Wolff, C.L., 1983, ApJ, 264, 667.

Wolff, C. L. 1992, SoPh, 142, 187

Wu, C.-J., Krivova, N. A., Solanki, S. K. and Usoskin, I. G. 2018, A&A, 620, A120

Yeo, K. L., Krivova, N. A., Solanki, S. K., Glassmeier, K. H. 2014, A&A, 570, A85

Yeo, K. L., Krivova, N. A., & Solanki, S. K., 2017, JGRA, 122, 3888

Zaqarashvili, T. V., Carbonell, M., Oliver, R., & Ballester, J. L. 2010, ApJ, 709, 749

Zaqarashvili, T. V., Oliver, R., Hanslmeier, A., Carbonell, M.,Ballester, J. L., Gachechiladze, T, Usoskin, I. G., 2015, ApJL, 805, L14

Zaqarashvili, T. V. and Gurgenashvili, E., 2018, Front. Astron. Space Sci., 5, 7

Zaqarashvili, T. V., Albekioni, M., Ballester, J. L. et al., 2021, Space Science Reviews, 217, 15

Zechmeister, M., & Kürster, M. 2009, A&A, 496, 577